Constraining the suitability of barium as an indicator of paleoproductivity in different environments

Raya Ivanova Stavreva

Thesis presented in fulfilment of the requirements for the degree of Master of Science in the Faculty of Science at Stellenbosch University.

Tesis ingelewer ter gedeeltelike voldoening aan die vereistes vir die graad Magister in Natuurwetenskappe in die Natuurwetenskappe Fakulteit aan die Universiteit Stellenbosch

Supervisor: Dr S. Fietz

Proposed date of award of degree: December 2020

DECLARATION

By submitting this thesis electronically, I declare that the entirety of the work contained therein is my own work, I am the sole author thereof (save to the extent explicitly otherwise stated), that reproduction and publication thereof by Stellenbosch University will not infringe any third party rights and that I have not previously in its entirety or in part submitted it for obtaining any qualification.

Abstract

Primary productivity is a vital factor in the global carbon cycle, as it regulates atmospheric carbon dioxide through sequestration. Therefore, climate change is largely dependent on the fluctuations in productivity. To develop effective climate models, past productivity must be reconstructed. There are a variety of established paleoreconstruction methods applied to aquatic environments, one of which is based on total organic carbon (TOC). TOC is a traditionally utilized proxy has been applied to modern and past aquatic environments, as it is the dominant component of biological material. However, its preservation is strongly influenced by oxidation and consequently degradation. Barium, especially in the form of barite, has become a promising tool, due to its refractory nature and positive linear relationship to organic matter. Its application to productivity reconstruction is primarily constrained to open ocean settings, with only rare utilization in coastal shelf or lacustrine environments. This study investigates the efficiency of barium or barium-bearing compounds as a paleoproductivity proxy in various aquatic environments (freshwater lake, peatland, coastal upwelling and Open Ocean). Barium concentration profiles were constructed in different sedimentary records by ICP-MS and XRF analysis. These barium profiles were compared to primary productivity proxies (TOC and chlorophyll degradation products), elemental proxies (C/N), isotopic proxies ($\delta^{13}C$) and Al concentration as an indicator for lithogenic input. Statistical analysis was applied to the datasets to comment on the relationship between barium and the productivity proxies. Scanning Electron Microscope (SEM) analysis was used to further assess whether barium has an affinity to biological cell structures or mineral precipitates. Our study showed that barium exhibited no significant positive relationship with any paleoproductivity proxy in the continental settings (lacustrine and peatland). However, in core 2 (North Namibian Cell, 20° 30 S) of the coastal upwelling environment, barium exhibited a strong and positive relationship with productivity. Therefore this study concludes that barium was not a suitable proxy for paleoproductivity in continental settings (lacustrine and peatland) and only exhibited potential suitability in one sediment core in the shallow marine (coastal upwelling cell) setting, which should be further explored. For future research, higher resolution is required for the application of statistical analysis, in order to better define the suitability of barium in different study locations.

Uittreksel

Primêre produktiwiteit is 'n belangrike faktor in die globale koolstofsiklus, aangesien dit reguleer atmosferiese koolstofdioksied deur sekwestrasie. Daarom, klimaatsverandering is grootliks afhanklik van die skommelinge van produktiwiteit. Ten einde effektiewe klimaatmodelle te ontwikkel, moet vorige produktiwiteit herbou word. Daar is 'n verskeidenheid van gevestigde paleoreconstruction metodes toegepas op water omgewings, waarvan een is gebaseer op totale organiese koolstof (TOC). Die TOC as tradisioneel gebruik gevolmagtigde is toegepas op moderne en verlede akwatiese omgewings, want dit is die dominante komponent van biologiese materiaal. Die bewaring daarvan word egter sterk beïnvloed deur oksidasie en gevolglik agteruitgang. Barium, veral in die vorm van barite, het 'n belowende instrument geword, as gevolg van sy vrolike aard en oënskynlike verhouding tot organiese materiaal. Die toepassing van produktiwiteit rekonstruksie is hoofsaaklik beperk tot oop oseaan instellings, met slegs skaars benutting in die kus rak of lacustrine en. Hierdie studie ondersoek die doeltreffendheid van barium- of bariumdraende verbindings as 'n paleoproductivity gevolmagtigde in verskeie wateromgewings (varswater meer, peatland, kusopwelling en Oop Oseaan). Barium konsentrasie profiele is gebou in verskillende sedimentêre rekords deur ICP-MS en XRF analise. Hierdie bariumprofiele is vergelyk met primêre produktiwiteitsgevolmagtigdes (TOC- en chlorofilaglegende agteruitgangsprodukte), elementêre gevolmagtigdes (C/N), isotoopgevolmagtigdes (113C) en Al-konsentrasie as 'n aanwyser vir lithogeniese insette. Regressie en statistiese analise is toegepas op die datastelle om kommentaar te lewer op die verhouding tussen barium en die produktiwiteitsgevolmagtigdes. Skandering elektronmikroskoop (SEM) analise is gebruik om verder te bepaal of barium 'n affiniteit vir biologiese selstrukture of minerale neerslag het. Ons analise het getoon dat barium geen beduidende positiewe verhouding met enige paleoproductivity gevolmagtigde in die kontinentale instellings (lacustrine en peatland) uitgestal het nie. In kern 2 (Noord-Namibiese Sel, 20 ° 30 S) van die kus-opwellingsomgewing het barium egter 'n sterk en positiewe verhouding met produktiwiteit uitgestal. Daarom kom hierdie studie tot die gevolgtrekking dat barium nie 'n geskikte gevolmagtigde vir paleoproduktiwiteit in kontinentale instellings (melkeen en peatland) was nie en slegs potensiële geskiktheid in een sedimentkern in die vlak mariene (kusopwellingsel) omgewing uitgestal moet word, wat verder ondersoek moet word. Vir toekomstige navorsing word hoër resolusie vereis vir die toepassing van statistiese analise om die geskiktheid van barium in verskillende studieplekke beter te definieer.

ACKNOWLEDGEMENTS

I would like to kindly thank Anson W. Mackay and Dr Andrea Baker for contributing data for the lacustrine (Lake Baikal) and peat (Mfabeni peatland) sample locations. I wish thank Ismael Kangueehi for contributing data for coastal marine (off-shore Namibia) sample location. I am grateful to Riana Rossouw, Mareli Groebbelaar-Moolman and Madelaine Frazenburg at the Stellenbosch University CAF lab, for preparing and processing sediment samples by ICP-MS, XRF and SEM analysis. I'm extremely grateful for my supervisor Dr Susanne Fietz, who has greatly assisted me these past two years. I am truly thankful for her constant support, dedication, and wise words. I cannot begin to express my thanks to my family and friends, who have always stood by me and cheered me on through all of this. I especially would like to thank my parents for supporting me in every way possible, thank you for always pushing me to be the best I can be.

Contents

List of figures

List of tables and equations

Chapter 1 Introduction

The consumption of inorganic carbon by marine primary producers and the subsequent conversion into organic matter is defined as primary production (Falkowski *et al.*, 2003). Primary productivity in turn is a vital factor in the global carbon cycle, as it is responsible for the sequestration of carbon from the atmosphere (Pfeifer *et al*., 2001). Primary productivity is thus related to climate change, as fluctuations of productivity influence the global climate through regulating the carbon dioxide concentrations in the atmosphere (Sageman, 2009). There is a growing concern of the impending effect of industrially induced climate change as there have been important variations of atmospheric carbon dioxide concentrations nowadays compared to those observed in paleorecords. Hence, it is crucial to recognise the interrelationship between production, marine geochemistry, atmospheric carbon and climate (Pfeifer, *et al*., 2001).

The reconstruction of paleoproductivity based on proxies recorded in sediments allows for the measurement of past carbon fluctuations within aquatic environments (Muller *et al*., 1979). Over the last few decades, there has been a variety of methods applied to reconstruct the paleoproductivity of many aquatic environments (Schoepfer *et al.*, 2015). For example, total organic carbon (TOC) is a traditionally utilized proxy for the reconstruction of the modern and past productivity of aquatic environments, as it is a dominant component of the biological material in the water column and sediment profile (Schoepfer *et al.*, 2015). However, TOC is strongly influenced by oxidation and consequently degradation (Henderson, 2002). This argues against the suitability of TOC as an adequate measure of productivity as it may reflect preservation (Schoepfer *et al.*, 2015).

Barium compounds, such as barite have been suggested as a more promising proxy, due to its refractory nature and apparent relationship to organic matter preserved in sediments (Liguori, De Almeida and de Rezende, 2016). The profile of barite concentration across sediment depth often corresponds to the profile of well-preserved and non-oxidized TOC (e.g., Martinez-Ruiz *et al.*, 2015). This has given support to studies that have utilised barite in order to reconstruct productivity in the water column, surface sediment and sediment profiles of marine environments (Dymond, *et al.*, 1992; Tribovillard *et al.*, 1996; Jeandel *et al.*, 2000; Pfeifer *et al.*, 2001; Babu *et al.*, 2002; Paytan *et al.*, 2003). Although it has been widely applied to open ocean settings, barium as a paleo-productivity proxy has rarely been studied in coastal shelf (Joung *et al.*, 2014) or lacustrine settings (Horner *et al.*, 2017).

Biogenic barium has been proposed for reconstruction mainly in marine environments, as the modern ocean is close to saturation with regards to barite and pelagic marine organisms are able to precipitate barite (Monnin *et al.*, 1999). However, some terrestrial spring and estuary environments that are sulphide rich and contain barium, are known to also produce biogenic barium (Stecher and Kogut, 1999; Senko *et al.*, 2004; Bonny and Jones, 2007). Nevertheless, pelagic barite precipitation has rarely been studied in freshwater systems that are undersaturated with respect to barite (Horner *et al.*, 2017). Some studies have been conducted in freshwater (Fritz *et al.*, 1990) and peat bog (Niedermeier, Gierlinger and Lütz-Meindl, 2018) where organisms such as protozoa, algae and clams are responsible for barite precipitation (Brook *et al.*, 1980; Rieder *et al.*, 1982; Finlay, Hetherington and Da Vison, 1983; Wilcock *et al.*, 1989; Gonza, Chekroun and Paytan, 2003). Due to the presence of barite forming freshwater organisms and the possibility of a biogenic formation of barite, there holds the question whether barium can be applied to non-marine settings such as freshwater systems.

Use of barium as a paleo-productivity proxy is not always apparent in various aquatic environments. For example, using barium as a productivity proxy for locations where intense

sulfate reduction takes places, must be considered with caution (Liguori, De Almeida and de Rezende, 2016). Sulfate reduction results in the migration of barium throughout the sediment profile (Tribovillard *et al.*, 2006) and therefore, may result in barium migrating during diagenesis and precipitating in sediment layers that were deposited with different concentrations of organic matter than the sediment layer it was originally deposited in (Tribovillard *et al.*, 2006). Hence results from one aquatic environment, such as the open ocean, cannot be directly extrapolated to applications in other settings, such as the above-mentioned coastal shelf or lacustrine environments. More research on the use of barium as paleo-productivity proxy in these specific settings is therefore still required.

1.1 Aims and objectives

The main aim of this study is to determine whether barium is a reliable paleo-productivity proxy in diverse range of environments including a freshwater lake, or whether it is constrained only to marine environments. Barium has extensively been explored as an alternative measure of primary productivity, but primarily within marine environments as compared to fresh water environments. Thus the main objective is to provide new data for a suite of environments ranging from freshwater to marine systems. Barium profiles are produced by applying ICP-MS and XRF analysis on sediment samples.

This study will begin by reviewing previously published literature on barium as a paleoproductivity proxy in marine and lacustrine environments. Through this review, the advantages and disadvantages of barium as a paleo-productivity proxy will be established within different environments. In the literature review, examples of successful applications of barium as a paleoproductivity proxy will be shown for the open ocean environment.

Following the literature review and the overview of open ocean environments, I will compare more established paleoproductivity data (Baker *et al.*, 2014; Mackay *et al.*, 2017) with the barium datasets of this study, in lacustrine, peatland and coastal environments. This is completed to understand whether barium profiles follow a similar distribution pattern as other productivity proxies in these diverse aquatic environments.

Lastly, it is vital to have a better understanding of how barium is introduced into sediments and how biogeochemical factors influence the formation of barite, i.e. how does barium reach the sediment and therefore how is it ultimately preserved. The aim in this final section is therefore to determine whether barium is precipitated by biological organisms such as phytoplankton, or whether it chemically precipitates and forms minerals such as barite in the different aquatic environments. This is achieved through SEM imaging analysis, whereby the composition and elemental species and distribution is examined.

Chapter 2 Literature review

2.1 Overview of sources and composition of sedimentary organic matter in different settings

Allochthonous and autochthonous material: Sedimentary organic matter represents the chief reserve of organic carbon in the total carbon cycle (Zonneveld *et al.*, 2010). In the ocean, organic matter is of allochthonous, terrestrial origin or it is generated by primary production (Kandasamy and Nath, 2016). Allochthonous organic matter that is sourced from continental settings, enters the marine system via fluvial and eolian processes (Burdige, 2007; Kandasamy and Nath, 2016). This organic material has been created through physical break-down and/or chemical transformations, therefore is it already altered when entering the water column (Hedges, Keil and Benner, 1997; Kandasamy and Nath, 2016). Autochthonous organic matter

is composed of degradation products of various biological organisms, such as plankton, including of primary producers in the surface waters (Meyers, 1997). Phytoplankton is responsible for the primary production and consumption of nutrients within the surface waters (Falkowski *et al.*, 2003). A minor portion, estimated at 1%, of organic matter is transported to the sediment (Liguori, De Almeida and de Rezende, 2016).

Impact of physical factors on deposition; Physical factors that greatly influence organic matter deposition and preservation include composition of the sinking particle, temperature of the water column and sediment texture at the site of ultimate burial, which impact how long the material's exposed to oxygen and other break-down agents (Ganeshram, 2006; Zonneveld *et al.*, 2010). Organic material contain a variety of aggregates that are either labile or refractory based on their molecular structures or physical forms (Hedges, Keil and Benner, 1997). The molecular structure of terrestrially sourced organic matter in marine sediments is reliant on the degradation processes within soils and the transport mechanisms, as both influence the organic material's degradation potential in the ocean (Zonneveld *et al.*, 2010).

Impact of biological factors on deposition: Biological communities of protozoans and metazoans are hosted within marine sediments and such organisms have a direct and indirect influence on the biochemistry of the sediment and how organic matter is processed (Zonneveld *et al.*, 2010). These marine animals, protists and microbes consume organic material, therefore they directly affect the transformation and production of organic matter (Hedges, Keil and Benner, 1997). They can also indirectly influence textural modification, biological deposition, biological irrigation and bioturbation. Bioturbation can cause the alteration of sediment properties, such as porosity, permeability and compaction of sediment (Meysman, Middelburg and Heip, 2006). Thus in turn resulting in a change of the organic matter- water column dynamics, which can cause the exposure of organic matter to oxidants. This can cause a change

in the redox environment, which therefore stimulates decomposition of organic matter (Canfield, 1994).

Preservation of organic matter in marine versus lacustrine environments: The preservation of organic matter can differ in different sedimentary environments such as lacustrine and marine settings. Due to the stark difference in size and age of marine and lacustrine environments, each has a distinct sedimentation pattern and chemical composition of organic material (Meyers, 1997). Lacustrine settings are generally smaller in size in comparison to marine settings, yet receive larger proportions of terrestrially sourced sediments (Gudasz *et al.*, 2010). Therefore the sedimentation rate in lakes is greater, resulting in a faster burial of organic matter (Dean and Gorham, 1998; Contreras *et al.*, 2018). Preservation of organic matter can be diminished in lacustrine settings by turbulence at the sediment floor, resulting in the resuspension of organic particles into the water column and subsequently exposure to oxygen (Meyers and Ishiwatari, 1993). The surface water layer of marine environments is abundant with dissolved oxygen, conversely the lower layers of the water column of lacustrine environments seasonally may become oxygen depleted and anoxic (Sobek *et al*., 2009). Dissolved oxygen in the water column can influence the degradation rate and the sort of degradation which organic matter experience (Sobek *et al*., 2009). Dissolved sulphate is one of the major ions of the marine water column (Griffith and Paytan, 2012), however it is not present in most lacustrine water columns (Millero *et al.*, 2008). The composition of marine organic matter is dependent on microbial modification as a result to sulphate reduction (Meyers, 1997).

Preservation of organic matter in coastal environments: As a result of all of the above mechanisms, the concentration of organic carbon is often greater within lacustrine sediments as compared to marine sediments (Dean and Gorham, 1998). The only other aquatic setting similar, with regards to sedimentation patterns and preservation of organic matter, to lacustrine environments is coastal marine settings (Meyers, 1997). Due to their shallow water column and

close proximity to land, there is a higher sedimentation rate of terrestrially-derived organic material and therefore accumulation and subsequently preservation of organic matter (Meyers, 1997).

2.2 Degradation, transportation and preservation of organic matter

An introduction into particulate, dissolved, refractory and labile fractions: Biological, physical and chemical parameters influence how organic matter is degraded, transported and eventually preserved over time (Hedges, Keil and Benner, 1997). Organic matter is present within the water column as a particulate and dissolved fraction (Figure 2.2.1), both composed of labile (easier to break down) and refractory (hard to break down) components (Burdige, 2007). Particulate organic matter (POM) is transported to the sediment floor through sedimentation or by sinking biological organisms (Zonneveld *et al.*, 2010). This organic material is composed of various constituents with varying quantities and reactivities, ranging from refractory to labile (Meyers and Ishiwatari, 1993). Refractory particulate organic matter (RPOM) can host some labile particulate organic matter (LPOM), which can be susceptible to biodegradation (Burdige, 2007). However, (RPOM) can become protected from degradation through encapsulation or by sorption onto inorganic particles (Zonneveld *et al.*, 2010). This labile fraction will be liberated once the particles they are attached to degrade or when it is desorbed from the particles (Zonneveld *et al.*, 2010).

Processes taking place with depth in the sediment: Deterioration of organic material occurs within the upper oxic section of the water and sediment profile at a fast pace. This degradation rate decreases exponentially as residual organic matter becomes more refractory after every degradation process (Meyers, 1997). The topmost sediment strata are inhabited by organisms which allow for the transportation of organic matter from underlying anoxic zones towards the

upper, oxic section by means of bioturbation (Hollerbach and Dehmer, 1994; Ganeshram, 2006). The underlying anoxic region of the sediment profile is made up of a sequence of redox zones, each with its own microbial communities consuming and producing unique types of organic matter (Wang *et al.*, 2019). This is due to the fact that, with sediment depth, there is a decrease in the available redox potential, which is the energy gained once organic matter deteriorates (Canfield and Thamdrup, 2009). As the potential for the energy gain declines, the rate of biotransformation decreases as some processes are no longer energetically viable (Fiedler, Vepraskas and Richardson, 2007). Subsequently, the organic matter that required these biotransformation processes in order for digestion to occur, is transported from the labile material phase and into the refractory material phase. This results in the accumulation of organic material within underlying sediments (Zonneveld *et al.*, 2010).

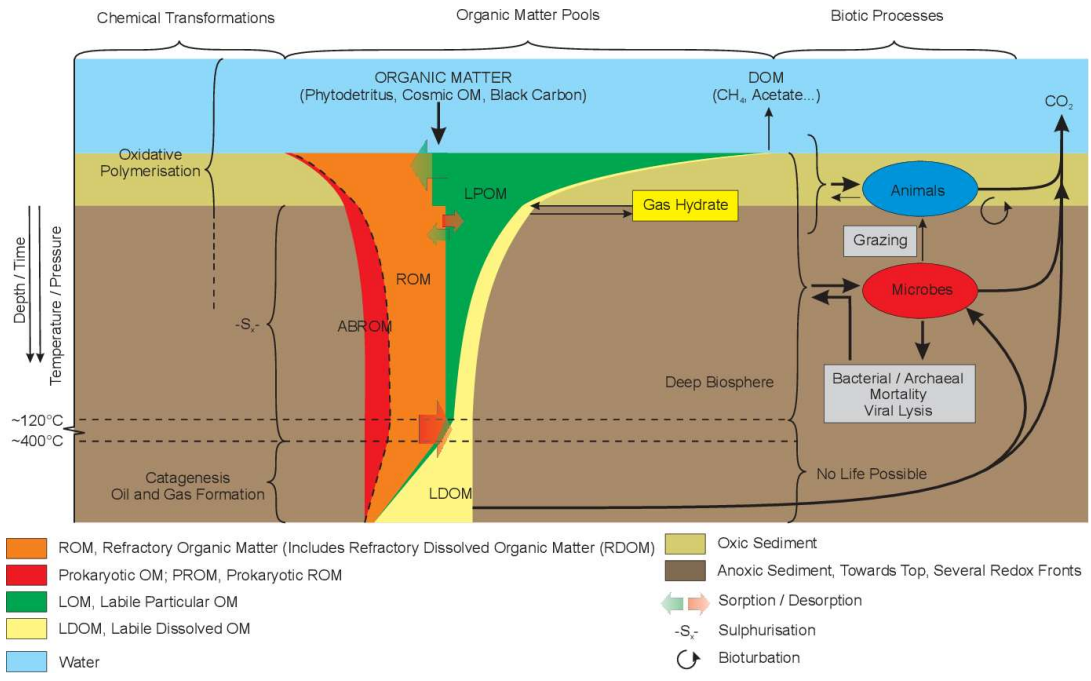

Figure 2.2 1: The transformation of organic matter through degradation processes in the water and sediment profile (modified from Zonneveld et al., 2010).

2.3 Primary productivity and total organic carbon

Primary production: Organic productivity is a vital parameter in aquatic environments, and is responsible for regulating biological dynamics, redox conditions, cycling of carbon and nutrient cycling. In the mixed surface waters of the water profile, the main primary producers of organic matter are single-celled phytoplankton (Falkowski *et al.*, 2003). Phytoplankton is responsible for the conversion of inorganic carbon, into organic matter through photosynthesis, thus this results in 'primary productivity' (Falkowski *et al.*, 2003). The extent of primary production depends on the accessibility of light intensity and nutrients, such as nitrate, phosphate and trace elements (Schoepfer *et al.*, 2015).

Export production: The portion of the total primary productivity that sinks out of the water surface layer, is defined as the export production (Tribovillard *et al.*, 2006). Degradation processes occur in the water column as well as in the sediment. In the upper water column, the descending particles are exposed to bacterial respiration, thus triggering a decomposition of the material before it sinks to the sediment floor (Schoepfer *et al.*, 2015). Only a small fraction of the decomposed material survives and is deposited on the sediment-water interface (Canfield, 1994). As has been outlined above (section 2.1 and 2.2), further degradation occurs within sediments. The portion of the organic carbon within the water column that sinks to the sediment and is preserved, is defined as the organic matter burial efficiency and is often recorded between 16 – 30 % in marine environments (Kandasamy and Nath, 2016). As outlined above (section 2.2.) this depends on the conditions in the sediment. For example, in reducing environments 30% of the primary production has been preserved, in comparison to only 1% recorded in oxic environments (Liguori, De Almeida and de Rezende, 2016).

Total organic carbon as proxy for paleo-productivity: Total organic carbon (TOC) is a traditionally utilized proxy for the reconstruction in aquatic environments (Tribovillard *et al.*, 2006). The TOC content of the sediment is a representation of the primary productivity, export

productivity and the preserved organic carbon within the water-sediment profile (Contreras *et al.*, 2018). However, as outlined above for organic matter (section 2.1, 2.2, 2.3), the carbon sediment profile can be remineralized as a result of exposure to bacteria that causes aerobic respiration (Schoepfer *et al.*, 2015). Hence, an elevated primary productivity of the surface water does not equate to a substantial total organic carbon content within sediments. The preservation of organic matter can be enhanced by way of decreasing exposure to oxygen, achieved via a reducing redox environment and rapid sedimentation (Ganeshram, 2006). A prominent relationship, between the accumulation rate of organic carbon and the preservation factor, holds within oxic modern aquatic environments. Thus, often, the higher the sedimentation rate, the greater the rate of preservation (Tyson, 2011). However, in suboxic and anoxic environments accumulation of organic carbon is not only dependent on the rate of sedimentation, because of a low exposure to oxygen and therefore higher rate of preservation of organic carbon (Schoepfer *et al.*, 2015).

2.4 Barium as a productivity proxy

Source of barium in aquatic environments and sediments: Barium (Ba) is a trace element originating from sedimentary and igneous rocks in the earth's crust (Liguori, De Almeida and de Rezende, 2016). It enters aquatic systems via chemical and physical weathering of these rocks and minerals. In the water column, barium is present in a dissolved or particulate phase (Figure 2.4.1)(Chow, Tsaihwa; Goldberg, 1976; Liguori, De Almeida and de Rezende, 2016). The relationship between the dissolved and particulate phase is dynamic, i.e. dissolution and precipitation processes both take place in the water column (Liguori, De Almeida and de Rezende, 2016). The amount of dissolved barium is partially dependent on the external, terrestrial (lithogenic) supply of particulate barium and the hydrodynamic conditions in the water column (Liguori, De Almeida and de Rezende, 2016). Barium is liberated from the lithogenic particulate fraction through ion exchange processes, where barium is exchanged

with another highly concentrated ion in the environment (Hanor and Chan, 1977; Coffey *et al.*, 1997).

In addition to the lithogenic fraction, such as oxy-hydroxides, carbonates and aluminosilicates, in the marine settings, particulate barium is primarily associated with sulphate (SO_4) forming barite (Figure 2.4.1) (Dymond, Suess and Lyle, 1992). Barite forms authigenically in the marine systems that are undersaturated (Tribovillard *et al.*, 2006). In order to form, barite requires the interaction of barium and sulphate super-saturated solution for it to precipitate and transport to the sediment, where it will eventually be preserved (Griffith and Paytan, 2012). Such barite can form upon the degradation of organic matter (Figure 2.4.1), where sulphur is oxidised to form sulphate resulting in a super-saturated micro-environment in which barite can form (Paytan and Griffith, 2007). As mentioned above, the relationship between the dissolved and particulate phase is dynamic: Barite remains stable in oxic sediments, but it becomes remineralized under reducing conditions (Figure 2.4.1) (Martinez-Ruiz *et al.*, 2015). Sediment conditions can evolve from oxic to reducing as a result of continuous deposition and organic matter decomposition (Shigemitsu *et al.*, 2007). This consequently results in the release of barium into the sediment pore water and the sediment-water interface (Tribovillard *et al.*, 2006).

Barium's relationship with productivity: Barium compounds are refractive, and better preserved than biogenic silica or organic carbon, and therefore are a promising proxy for paleoproductivity (Dymond et al., 1992) hence, the great interest in defining the mechanisms of the barite-primary productivity relationship. The dissolved barium concentrations within aquatic environments are minimally attributed to direct hydrological, biological and terrestrial sources, but rather may have originated from recycled biogenic material (Pfeifer, Kasten, Hensen and Schulz, 2001). This is compatible with the idea that barium has strong ties with productivity, as it is the result of the dissolution of residual biogenic debris

(McManus *et al.*, 1994). This is supported by the fact that dissolved barium is characteristically scarce in surface waters and abundant in deep water, with increasing concentrations as depth increases, thus it displays a nutrient-like distribution in the water column, indicating a direct and indirect influence by the biological organisms through uptake and re-mineralisation (McManus *et al.*, 1994). The distribution of dissolved barium, particulate organic carbon and organic debris display a positive linear relationship in the water profile. Many studies (Dymond *et al*., 1992; Francois *et al*., 1995; Tribovillard *et al*., 1996; Kasten *et al*., 2001; Riquier *et al*., 2005) have utilised the relationship between the uptake of dissolved barium and sinking of particulate organic carbon, as a potential indicator for paleoproductivity. Nonetheless, the correlation between biogenic barium and particulate organic carbon has been disputed, as some argue that this relationship is only an artefact of biological filtering and packaging, i.e. a common carrier (Paytan and Griffith, 2007).

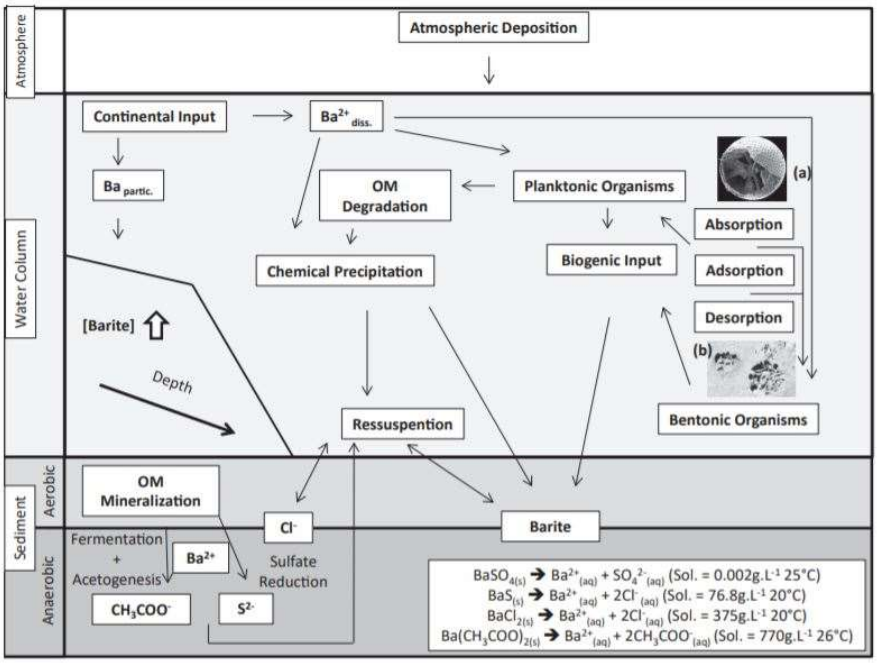

Figure 2.4.1: The deposition of barium, formation mechanism of barite within the water column and transport between the sediment-water interface (modified from Liguori, De Almeida and de Rezende, 2016).

2.5 Previous application of barium contents to reconstruct primary productivity

As mentioned before (chapter 1), barium compounds, such as barite have been suggested as a more promising proxy than previously established (e.g. TOC), due to its refractory nature and apparent relationship to organic matter preserved in sediments. The theory that barium is a more reliable productivity proxy rests on the idea that the distribution profile of barite (barium) concentration across sediment depth often correlates and displays a linear relationship with organic matter. Dymond, Suess and Lyle (1992) for example, collected sediment trap samples and studied respective fluxes in three marine settings (California coastal upwelling current, the Equatorial pacific and the Atlantic). The aim of Dymond, Suess and Lyle (1992)'s study was to evaluate the relationship between organic carbon and barium; and the degree of preservation of barium in sediment. Dymond, Suess and Lyle, (1992), devised a formula where the excess barium (the biogenic barium portion of the total barium content) is calculated from terrigenous material in the sediment. The biogenic barium fraction exhibits a positive linear correlation to organic carbon (Figure 2.5.1), and thus it is a good indicator for productivity within the sediment profile (Dymond, Suess and Lyle, 1992).

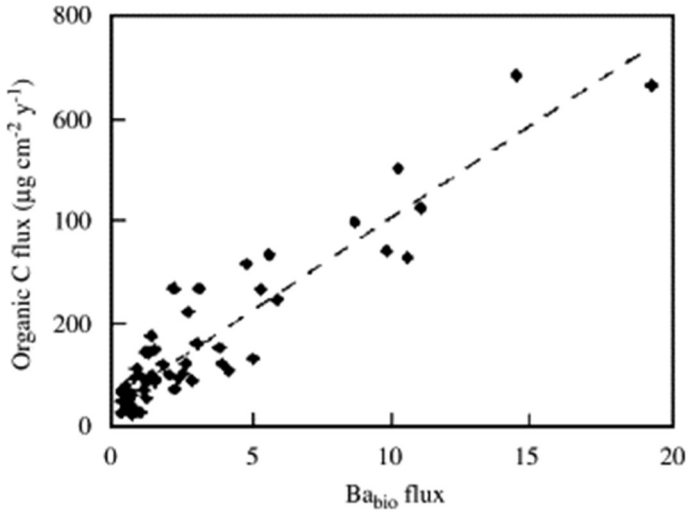

Figure 2.5.1: The linear relationship between biogenic barium and organic carbon fluxes, from 10 sediment traps in various marine environments (modified from Dymond, Suess and Lyle, 1992).

Similarly, Pfeifer, Kasten, Hensen and Schulz, (2001) investigated the concentration of barium within surface sediments of the South Atlantic, in order to reconstruct the primary production (Figure 2.5.2). This study, similar to Dymond, Suess and Lyle, (1992), utilizes the biogenic fraction of barium as potential productivity proxy. The ratio of organic carbon to biogenic barium was formulated from the concentrations of barium and organic carbon in surface sediments. This data was compared to previously published literature by (Dymond, Suess and Lyle, 1992; Francois, Manganini and Ravizza, 1995). The distribution of biogenic barium in the water column exhibited good correlation with primary productivity of the South Atlantic Ocean (Figure 2.5.2).

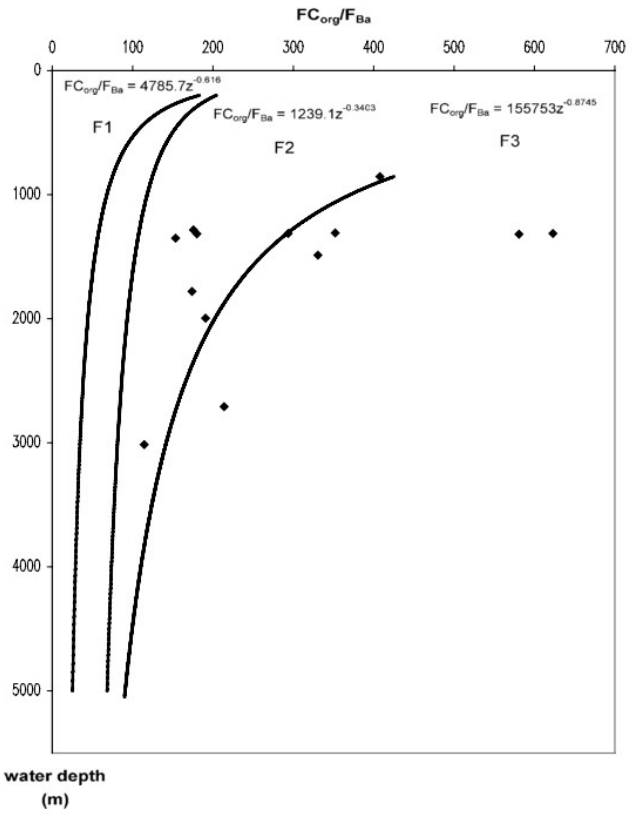

Figure 2.5.2: The ratio of organic carbon and biogenic barium throughout the depth profile from sediment trap data (modified from Pfeifer, Kasten, Hensen and Schulz, 2001).

Chapter 3 Study locations

The suitability of barium as a principle paleoproductivity proxy is tested over various aquatic environments. The sampling locations include a pristine continental lacustrine environment (Lake Baikal), which is devoid of any direct seawater influx. Similarly, a fen (Mfabeni peatland) is studied as it is similar to a lacustrine environment yet it may have had some marine influence in the past. Lastly, I include a shallow coastal offshore environment (Namibian up-welling cells).

3.1 Continental environment: Lake Baikal

3.1.1 Study site

Lake Baikal, the world's deepest (1642 m), largest (23 000 Km^2) and oldest lake is located within the South-Eastern mountainous region of Siberia, North of the Mongolian border (Colman, Karabanov and Nelson, 2003) . The lake is contained within an intracratonic rift basin that formed as a result of the Baikal Rift zone. This freshwater lake is underlain by a thick sequence of complex sedimentary records of continental environmental history spanning 25 million years (Fagel and Boës, 2008). Morphology divides the lake (Figure 3.1.1) into 3 sub-lake basins (the South, Central and North Baikal Basins) which are disconnected by interbasin highs (the Selenga Delta and the Academician Ridge) (Charlet *et al.*, 2005). This study focuses on the Vydrino shoulder isolated high within the southern sub-basin (Figure 3.1.1). The isolated high is an elevated ridge, at a height of 800m below water depth, which is distant from basin floor disturbances such as turbidity flows, base water currents and river inflow disturbances.

The lithological succession of the sediment cores CON01-605-5 (Vydrino Shoulder) is hemipelagic in composition (Charlet *et al.*, 2005).

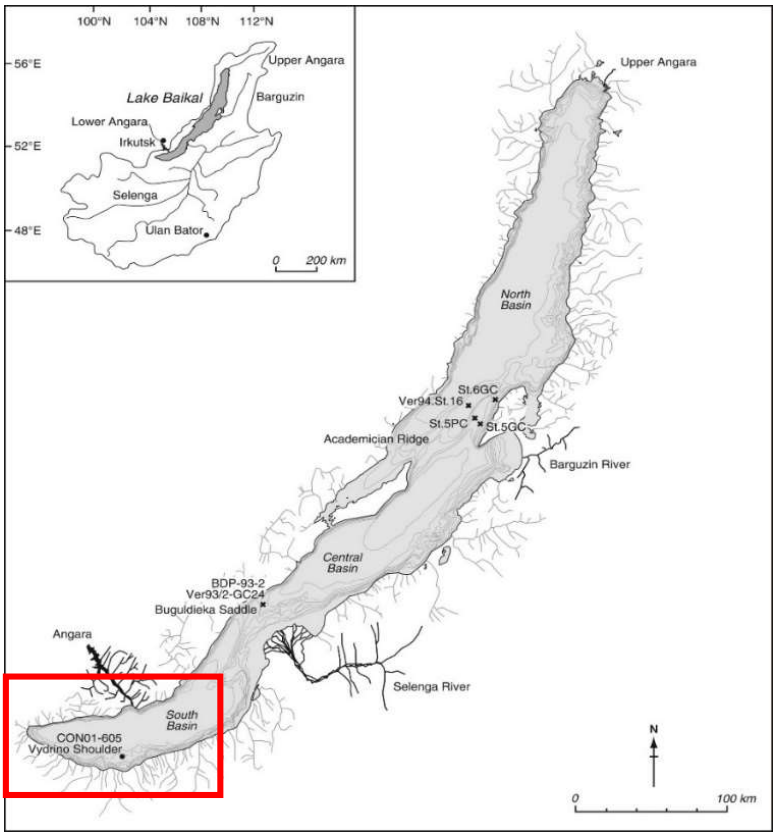

Figure 3.1.1: Map of the Lake Baikal catchment area with various study sites, including the Vydrino Shoulder (CON01-605-5) of the southern sub-basin, which is represented by the red square (modified from Charlet *et al.*, 2005).

3.1.2 Geology and composition

Lake Baikal is positioned on an active continental rift in south eastern Siberia defined as the Baikal Rift Zone. This rift parts the Siberian craton in the northwest and the Mongolian–Transbaikalian Belt in the southeast (Och *et al.*, 2014). The rifting began during the Oligocene (34–23 Ma) and is responsible for the construction of the deepest lake, which is filled with a sediment thickness of 10km (Och *et al.*, 2014). The South basin of Lake Baikal is primarily fed by two sources, the Angara River and the Selenga Delta. The watershed geology of the

respective rivers is composed of exposed granitoid, Precambrian metamorphic rocks and quaternary soil cover (Och *et al.*, 2016). Thus these characterise the principal suppliers of the allochthonous material deposited in the lake (Och *et al.*, 2014). The Vydrino Shoulder is located along the Hamar-Daban Highland range and alee the Angara Tributary (Colman, Karabanov and Nelson, 2003). Its morphology forms an upper to mid-sloped terrace adjoining the coast and a gentler slope near the deep basin floor (Colman, Karabanov and Nelson, 2003). The shoulder is a terrace carved by canyons, to depths of 300m and affected by fault activation (Demory *et al.*, 2005). The ridge crest displays flatter and continuous morphology. The lithology of the ridge is comprised mainly of fine grained sediments of detrital muds with a rich diatom layers in the upper units of the sediment profile (Charlet *et al.*, 2005). The upper portion of the core is dominated by silty clay to clayey silt lithology with highly concentrated and greatly diverse diatoms species. Their concentration and diversity decreases gradually with increasing depth. The core hosts repeated layers of decametric yellowish-sand (Charlet *et al.*, 2005).

3.1.3 Hydrology and sedimentation

Lake Baikal's catchment area and surrounding tributaries are sparsely inhabited which results in only minor anthropogenic pollution. The river input into Lake Baikal equates to 58 km^3 per year with a carrying capacity of roughly 4000 kt of suspended particulate matter per year. The Selenga River is the primary water and particle source into the lake, followed by the Upper Angara River which flows into the northern tip of Lake Baikal (Heim *et al.*, 2005). The composition of the suspended material deposited by the two rivers is vastly different. The Selenga River load is mainly composed of lithogenic elements and it deposits 80% of all the aluminium inflowing the lake. Whereas the Angara River greatly influences the redox sensitive elements such as iron within the lake.

3.1.4 Previous reconstruction studies

Due to Lake Baikal's intercontinental location and sparsely populated surrounding regions, it is a pristine natural environment with an extensive historical record dating back millions of years. Such records are valuable for reconstruction objectives, as the lake's sediments host a wide variety of proxies that have been utilised in past studies in order to document the environmental changes as feedbacks to global changes. Expeditions to Lake Baikal for investigation of sediment composition and water chemistry began in the early 1970's (Falkner *et al.*, 1997). More recently studies have focused mainly on the use of proxies in order to reconstruct the paleo environmental and the paleoclimate of the lake Baikal region of Siberia, with a principle emphasis on reconstructing the transitioning environmental from the last glacial maximum period through to the Holocene. The most recent paper by Mackay *et al.* (2017), concentrates on the reconstruction of the South sub-basin with a multi-proxy approach based on lake sediments, in order to gain an improved understanding of the carbon dynamics of the region and how they may vary in future due to climate change sensitivity. The focal purpose of the Mackay et al. (2017) study is to recognize the climatic forcings of carbon dynamics throughout the warming and cooling events of the Late Quaternary, the influence of climatic events of the scale Milankovitch cycles and smaller, and the quantity of carbon that had been stored within Lake Baikal during the Holocene. There is evidence that more carbon content was buried in the early Holocene compared to the Neoglacial interval. Mackay *et al.* (2017) displays the close linkage between hydrological systems and the cycling of carbon within a system based on paleoenvironmental fluctuations.

3.2 Continental environment: Mfabeni peatland

3.2.1 Study site

The UNESCO Heritage iSimangaliso Wetland Park is located on the north end of the Kwazulu-Natal province of South Africa (Baker *et al.*, 2014). The park hosts the continent's largest estuarine system, Lake St Lucia (Figure 3.2.1). Lake St Lucia is an open surface waterbody that spans an area of $350Km^2$ with a north-south position and an average depth of 90cm throughout (Baker *et al.*, 2014). The northern coastal plain of KwaZulu-Natal is defined as Maputaland, and hosts a subtropical climate, with dry winters and wet, humid summers (Miller *et al.*, 2019). The eastern portion of the Maputaland primary aquifer is comprised of coastal sand dunes and low-lying plains (Grundling *et al.*, 2013). There are many varieties of wetlands prevalent in this region, from seasonally flooded depressions to continuous peatlands and marsh forests, whereas the terrestrial portion of this region is dominated by coastal dune forests and wooded grassland (Taylor *et al.*, 2006). The primary land use activities of this area are tourism and wildlife conservation (Baker, Routh and Roychoudhury, 2016). In close proximity to the eastern coast of Lake St Lucia, lies the Mfabeni peatland (Figure 3.2.1), which is enclosed by the Indian Ocean and is hosted within the Mkuze River catchment (Grundling *et al.*, 2015). The peatland is 10km long, 3km wide and covers a 1462 ha triangular area (Grundling *et al.*, 2013). The north and east ends of the marshland are overgrown with reed and sedge vegetation and the south and west end are dominated by swamp forest which extends into the central area of the peatland (Miller *et al.*, 2019).

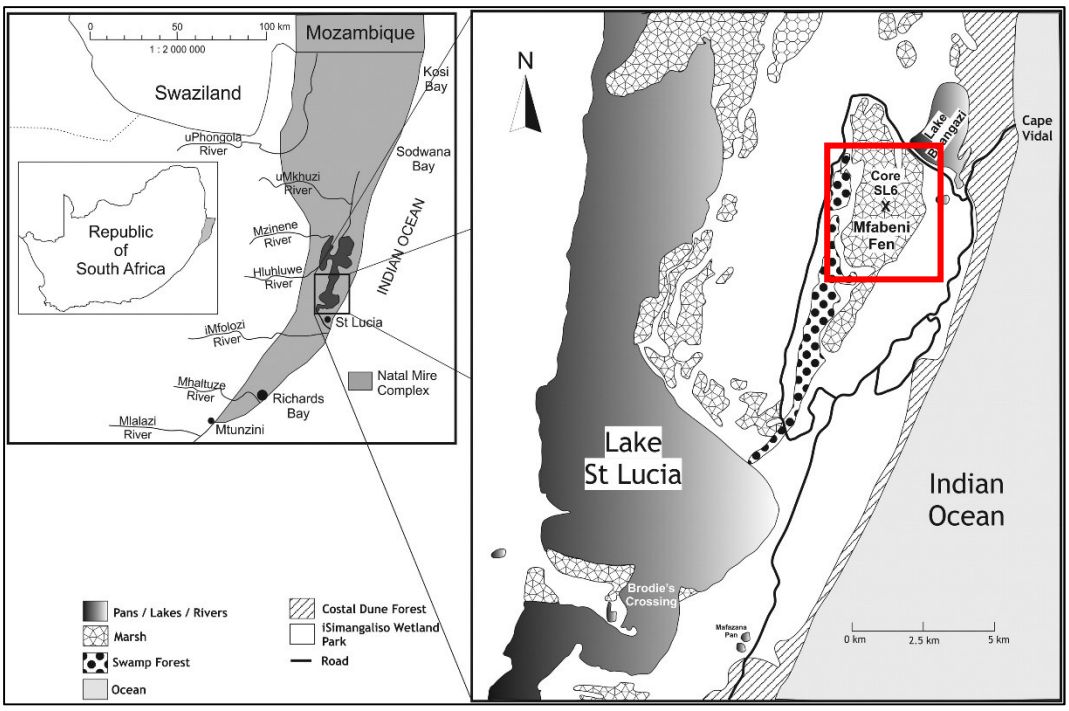

Figure 3.2.1: Sampling site (core SL6) represented by red square, Mfabeni peatland, Kwazulu-Natal, South Africa (modified from Baker, Routh and Roychoudhury, 2016).

3.2.2 Geology and composition

The regional geology is composed of rhyolite and basalt bedrock derived from the Lebombo range, this sequence is overlain by the Zululand group which is primarily composed of siltstones (Grundling *et al.*, 2013). There is a discontinuity in the stratigraphic structure between the siltstones and the overlying younger Port Durnford Formation which is comprised of lacustrine muds and clayey carbonaceous sand (Grundling *et al.*, 2013). This formation is overlain with well sorted, highly porous and permeable sands and sandstones form the Sibayi and KwaMbonambi formations (Grundling *et al.*, 2013). The KwaMbonambi formation develops into the lower western dune ridge, whereas the Sibayi formation forms the eastern coastal dune ridge. This structure results in the formation of the Mfabeni peatland (Taylor *et al.*, 2006). The Mfabeni peatland is a vast marshland that hosts a paleorecord that ranges from the Palaeolithic period (~45 kyr ago), onto a base layer of clay within an incised valley

depression containing reworked dune sands (Taylor *et al.*, 2006). The morphology of the Mfabeni peatland is complex and forms a deep centralized depression with a north-south orientation, surrounded by smaller depressions in the eastern and western portions of the main peatland (Grundling *et al.*, 2013). The primary peat basin is 10.8m thick with the surrounding depressions amounting to only a 2.5 m thickness (Clulow *et al.*, 2013). The surface of the peatland has a downward slope from the centre towards the south end. This results in a sloped water table ranging from the Mfabeni peat to the western dunes and from the peatland to the Indian Ocean (Miller *et al.*, 2019). In the northern and eastern ends of the peat, where sedge and reeds are hosted, the water table gently grades downwards to the east and suddenly drops between the east end of the marshland and the coastal dune area (Clulow *et al.*, 2013).

3.2.3 Hydrology and sedimentation

Precipitation is the primary source of water in the catchment area (Chaudhary, Miller and Smith, 2016). Majority of the annual rainfall occurs during the summer months, with precipitation ranging between 900 and 1200 mm per year, with the most of the rainfall concentrating on the western coastal dune area and decreasing towards Lake St Lucia (Taylor *et al.*, 2006). The Mfabeni peatland basin is seasonally recharged with an accumulation of water during the rainier summer season and declines in water levels during the drier winter season (Baker, Routh and Roychoudhury, 2016). Surface drainage is sourced from the Nkazana River and Lake Bangazi, depending on the water level of the lakes (Miller *et al.*, 2019). The main supply of groundwater to the Mfabeni peatland is by the swamp forest seepage area and the dune complex in the west end of the peatland (Grundling *et al.*, 2013). The central region of the marshland is recharged by surface water flows, which also recharge the shallow subsurface layers along its eastern border of the marshland (Finch, 2005). It is assumed that contribution of deep groundwater recharge is limited, therefore the marshland is dependent on the surface

and subsurface recharge flows for maintaining its functions. This results in seasonal accumulation of water in the Mfabeni basin during the wetter summer months and a groundwater level at/below surface soil during the drier winter months (Baker, Routh and Roychoudhury, 2016). The Nkazana River is responsible for capturing the surface water of the southern end of the marshland, and drains the water towards Lake St Lucia (Clulow *et al.*, 2013). The Mfabeni peatland hydrology and salinity variations are greatly dependant on evapotranspiration and precipitation of the area, due to its large surface area in comparison to its depth (Baker, Routh and Roychoudhury, 2016). The wet summer season brings about a freshwater composition on the northern end of the marshland, due to increase riverine input. Whereas, the southern end of the Mfabeni peatland is influenced by the estuary mouth, resulting in a more saline composition. However, over the dry winter months, salinity of the marshland increases as freshwater water input declines (Taylor *et al.*, 2006).

3.2.4 Previous reconstruction studies

Peatlands function as sinks for atmospheric carbon, sources of methane and producers of dissolved and particulate organic material (Baker, Routh and Roychoudhury, 2016). They are responsible for connecting short and long term carbon reservoirs (Baker *et al.*, 2014). Peat accumulations are suitable archives for paleoreconstruction studies based on their strong preservation rate and because they are deposited via autochthonous systems, which are dominated by climatic changes (Baker, Routh and Roychoudhury, 2016). Research on peatlands and the mechanisms that control carbon cycling between the atmosphere and sinks, has generally been focused within the Northern hemisphere on temperate/boreal peatlands (Gorham, 1991; Clymo, Turunen and Tolonen, 1998; Fenner, Freeman and Reynolds, 2005; Limpens *et al.*, 2008; Wania, Ross and Prentice, 2009). However, some recent studies (Finch

and Hill, 2008; Grundling *et al.*, 2013; Baker *et al.*, 2014, 2017; Baker, Routh and Roychoudhury, 2016) have focused on reconstructing the hydrological, environmental and peat forming variations in response to the changing climate in sub-tropical peatlands (Baker et al., 2016). The study of Baker *et al.* (2014) utilizes a suite of elemental (C/N, TOC, carbon accumulation rate) and stable isotope ($\delta^{13}C, \delta^{15}N$) proxies in order to reconstruct the past influences on the accumulation of carbon and organic matter along the Mfabeni sub-tropical coastal peatland. The multiple proxy approach resulted in the reconstruction of the source of organic matter, the preservation and diagenetic processes influencing the organic matter and the primary productivity. Such factors contributed to the formation of the peat deposits, and understanding their variations aid in the understanding of the paleoenvironment over the peatland in the last ~47 kyr before present (Baker *et al.*, 2014).

3.3 Coastal marine environment: upwelling cells offshore Namibia

3.3.1 Study site

Coastal upwelling systems contribute only 1% to the total area of the world oceanic system, however they are largely responsible for the global primary productivity (Silió-Calzada *et al.*, 2008). The east-boundary current system located offshore Angola, Namibia and South Africa is defined as the Benguela upwelling system (Figure 3.3.1)(14°S - 36°S, ~10°E – 22°E), and is one of the four main coastal upwelling zones of the global ocean system (Silió-Calzada *et al.*, 2008). The Benguela upwelling region is ~200km wide and extends over 600 km offshore. The upwelling system is bound by the Benguela surface current that flows towards the equator along the Namibian shore (Emeis *et al.*, 2018). The warm Agulhas and Angola currents confine the cool Benguela current at the southern and northern end respectively (Nardini *et al.*, 2019). The southeast trade winds control the wind pattern along the south western coast of Africa, driving the Benguela current and the offshore transport of shallow surface water (Zhao *et al.*, 2019). The combination of the Benguela current and the Southeast trade winds are responsible for the nutrient-rich South Atlantic Central Water mass in the Benguela upwelling region (14°S –36°S)(Silió-Calzada *et al.*, 2008)

The coastal orientation, topography, pressure and wind are the key factors responsible for defining the magnitude and strength of the Benguela upwelling system. The Benguela upwelling system can be divided into three regions, the northern (north of 25°S), southern (south of 30°S) and central (between 25°S and 30°S) Benguela upwelling systems (Barange, Pillar and Hutchings, 1992). The southern Benguela upwelling region is greatly impacted by the seasonal variability of the southeast trade winds, where little upwelling occurs during the winter months (June to August) due a northern shift in the South-east high pressure anticyclone

(Silió-Calzada *et al.*, 2008). The northern Benguela upwelling region is consistent and displays a maximum during the autumn/spring months (April to November) (Silió-Calzada *et al.*, 2008).

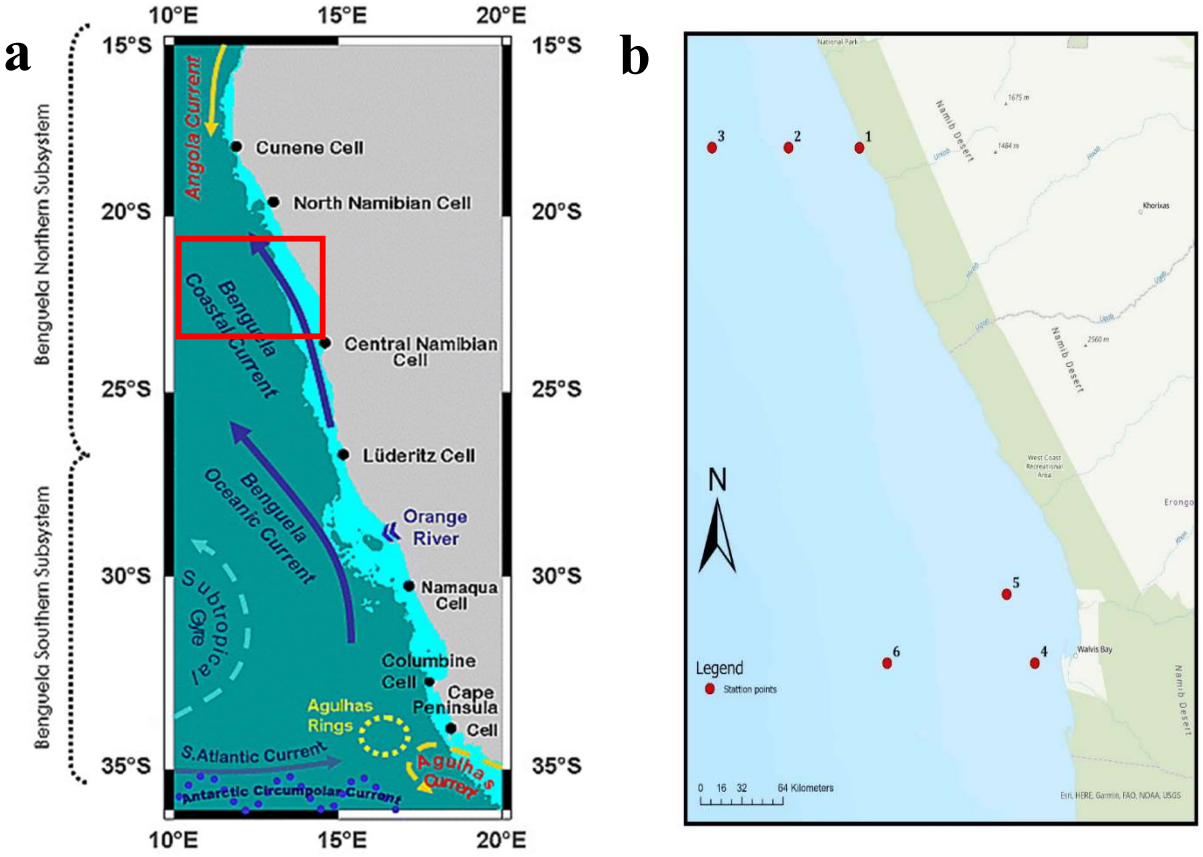

Figure 3.3.1: (a) Map of the Northern and Southern Benguela upwelling system along the NW shore of Southern Africa. The continental shelf (500m) is represented by the light blue area (modified from Silió-Calzada et al., 2008). (b) Map of the core sample locations along the cruise tracks 20° S and 23°S, which is represented as the red square in figure (a).

3.3.2 Geology and sedimentation

The Namibian region is characterized by margin development which is related to the Late Jurassic opening of the South Atlantic. Early margin development initiated with magmatism as a result of rifting, which can be observed today through the volcanic structures of the Etendeka flood basalt province and intrusive complexes such as the Erongo Mountains (Kukulus, 2004). The present Namibian morphology has resulted from uplift and erosion, subsequently creating the Great Escarpment that separates a deeply eroded coastal plain from the elevated hinterland (Kukulus, 2004). Off the North-western shore of Namibia lies the Walvis basin, a Cretaceous depositional centre that stretches a 100 000 km^2. The coastal basin displays a distinctive passive margin post-rift sediments in a wedge-shaped geometry (Kukulus, 2004). The Walvis basin is bounded in the north by the Walvis Ridge (~ 19.5° S), which is linked to the continental shelf by a shallow sill intrusion (~ 2500 m) defined as the Walvis Plateau (Mollenhauer *et al.*, 2002). The marine basin varies in width and depth, hosting several shelf breaks predominantly near the Walvis Bay area (23° S) (Mollenhauer *et al.*, 2002).

There is a substantial compositional variety of underlying sediments in this region. Sediments host great concentrations of organic carbon and biogenic opal, typical indicators of a high productivity area (Lazarus *et al.*, 2006). Organic carbon and opal enrichment in sediments is first recorded in the Late Miocene, thus indicating the initiation of the Benguela upwelling system (Lazarus *et al.*, 2006). Coastal sedimentation occurs at water depths of less than 150m, where diatoms generate an organic-rich 14 m thick secretion along the coast, extending 100km east-west and 700 km north-south (Emeis *et al.*, 2009). The sedimentation rates of the coastal upwelling diatomaceous mud belt are of the order of 1cm per 10 yrs (Emeis *et al.*, 2009). Two main perennial rivers are in the Northern Benguela that discharge sediment from the arid Namibian region into the coastal marine water column. These are the Kunene River in the

North (17° S) and the Orange River in the South (29° S), with discharge rates of 6.8 km^3 per year and 11 km^3 per year respectively (Holzwarth, Esper and Zonneveld, 2007). Another terrestrial input into the coastal upwelling cell is through the Southeast trade winds, which are responsible for transporting aeolian dust from the Namib and Kalahari deserts into the coastal marine area (Holzwarth, Esper and Zonneveld, 2007).

3.3.3 Hydrology

Due to the constant input of nutrients into the euphotic zone by upwelling mechanisms, the investigated study sites in the Benguela upwelling system experience a high productivity. Diatoms typically dominate the phytoplankton community, with some phytoplankton blooms also dominated by coccolithophores (Siegel *et al.*, 2007). Near the coast the diatoms are very abundant (concentrations greater than 10^6 cells per litre), however this concentration swiftly decreases (to 10^2 cells per litre) over the continental slope (Emeis *et al.*, 2009). The primary productivity in the Northern Benguela upwelling region is 1.2 g C/m^2/day (Emeis *et al.*, 2009), and is dependent on the nutrient supply to the area. Characteristic concentrations of nutrients in the upwelling zone include nitrate (15-25 µM), phosphate (1.5- 2.5 µM) and silicate (5- 20 µM) (Emeis *et al.*, 2009). These concentrations increase on the shelf to, nitrate (10-30 µM), phosphate (2- 3 µM) and silicate (20- 50 µM) (Emeis *et al.*, 2009); however they decrease in the pelagic water over the continental slope to, nitrate (< 5 µM), phosphate (< 21 µM) and silicate (< 1 µM) (Emeis *et al.*, 2009).

Dissolved oxygen becomes depleted towards the bottom of the water column, as bacteria deplete the oxygen while decomposing the sinking organic material (Pitcher, Brown and Mitchell-Innes, 1992). Hydrogen sulphide is produced in these sub-oxic to anoxic deep waters, as a result of sulphate reduction and denitrification processes (Siegel, Ohde and

Gerth, 2014). As the Southeast trade winds create Ekman transport offshore, so the deeper marine currents in the water column transport hydrogen sulphide rich waters towards the shore (Siegel, Ohde and Gerth, 2014).

However, there are mechanism that supply oxygen to the shelf water masses off the shore of Namibia. The South Atlantic Central Water mass is a compensation undercurrent that flows poleward, and works against the effect of the Ekman transport (Emeis *et al.*, 2018). This water mass mixes with the oxygen-depleted deep waters of the Northern Benguela upwelling cell (Hutchings *et al.*, 2009) and delivers water with a concentration of up to 90 µmol O_2/L to the northern coast of Namibia (Emeis *et al.*, 2009). The Eastern South Atlantic Central Water mass is another compensation current to the Ekman transport, however it is transported towards the Namibian shore in surface waters via advection. The mixing of the water masses results in oxygen enrichment of 178 µmol/L (Emeis *et al.*, 2009). The oxygen enrichment depends on the position and strength of the Southeast trade winds, which subsequently affect the fluctuations in the strength of the upwelling system and the composition of the mixing water masses (Emeis *et al.*, 2018). Therefore there is a higher need of oxygen when the Southeast trade winds weaken, which results in still water masses and the subsequent promotion of phytoplankton blooms (Emeis *et al.*, 2009).

Chapter 4 - Materials and Method

4.1 Continental environment: Lake Baikal

4.1.1 Sample collection and preparation

The Vydrino sediment core (CON01-605-5) of Lake Baikal was previously collected in the South sub-basin during the 2001 summer expedition. The box core (CON01-605-5) was extracted from the peak of an isolated high ridge, which is in close proximity to the shoreline of the South sub-basin (section 3.1). The ridge structure displayed a continuous and uninterrupted sedimentation history (section 3.1). The top few centimetres of the box sediment core was not archived, which results in the lack of reconstruction of the recent 800 years. The samples (CON01-605-5), collected for this study had previously been processed and prepared by milling and freeze-drying, I have further homogenized each sample by use of a mortar and pestle. For the purposes of my own study; chlorin, ICP-MS and XRF analyses (described below) were applied to the samples.

4.1.2 Core Description

The core (Figure 4.1.1) shows alternating green-tinged muddy clays and deep olive green biogenic diatom-rich intervals. There is also a substantial abundance of detrital material throughout the sediment profile, which reflects strong influence of fluvial inputs (Charlet *et al.*, 2005). The lithology of the ridge is comprised mainly of fine grained sediments of detrital muds with a rich diatom layers in the upper units of the sediment profile (Figure 4.1.1). The upper portion of the core is dominated by silty clay to clayey silt lithology with highly concentrated and greatly diverse diatoms particles. Their concentration and diversity decreases gradually with increasing depth (Charlet *et al.*, 2005).

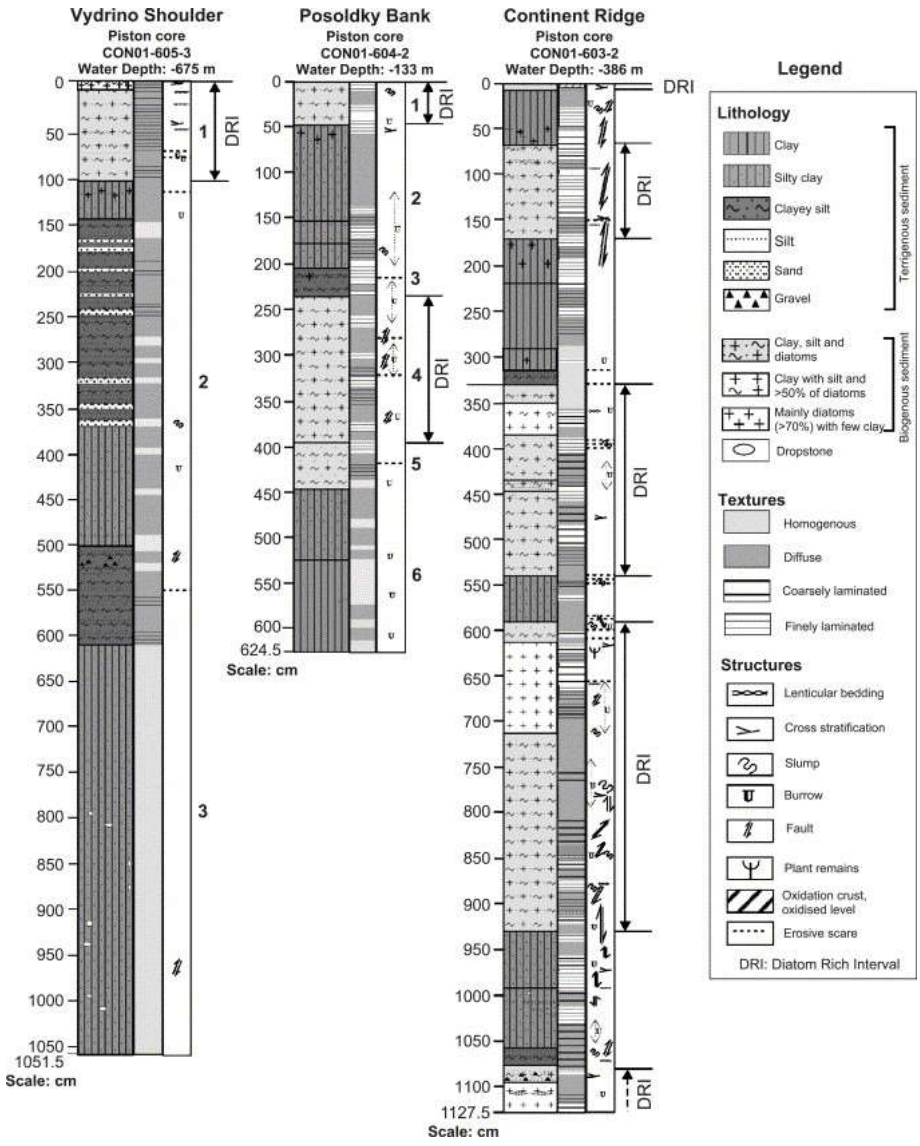

Figure 4.1.1: Stratigraphy of Lake Baikal Southern sub-basin cores, Vydrino Shoulder and Polsoldky Bank, (modified from Charlet et al., 2005).

4.1.3 TOC data and Chlorin analysis

The record of primary productivity of Lake Baikal is studied through chlorin analysis and TOC records. The TOC data were obtained from Prof Anson Mackay (University College London) as published in (Mackay et al., 2017). I conducted the chlorin analysis for this study and applied it to quantize the content of chlorophyll-a degradation products. Chlorophylls are pigments for photosynthesis in green plants and phytoplankton, providing the cells with energy sourced from sunlight to convert inorganic carbon into organic carbon. This indirect measurement of past lake productivity is expressed as the chlorophyll-a degradation products (chlorins, standing for biomass) per gram sediment. The chlorin analysis includes an extraction stage, where 4ml of acetone is added to 1g of sediment in a sample vials, and mixed utilizing a vortex. The vials containing the sample mixture are then submerged into an ultrasound bath filled with ice water, for 15 minutes. After ultrasonication, samples are placed in a dark and cold refrigerator to extract overnight. After a minimum extraction time of 24 hours in the refrigerator, the samples are centrifuged at 2000 rpm for 5 minutes in order to separate the solvent from the sediment. The sampling tubes are removed gently out of the centrifuge equipment without disturbing the settled sediment. Using a glass Pasteur pipette, the supernatant from the sample tubes is placed into a new sampling vial. The samples are then analysed, whereby 1ml of supernatant of the sample tube is decanted into a quartz cuvette and the absorption of the sample is measured by a spectrophotometer at 665nm wavelength. A Sigma-Aldrich chlorophyll-a standard was used to produce several different chlorophyll-a concentrations (1µg/L, 10 µg/L, 50µg/L, 250µg/L and 500µg/L). These chlorophyll-a concentrations were plotted against the measured adsorption values, in order to construct a calibration curve (Figure 4.1.2). A linear regression equation of $y= ax+b$ is applied to the graph (Figure 4.1.2), from which the chlorin concentration can be calculated.

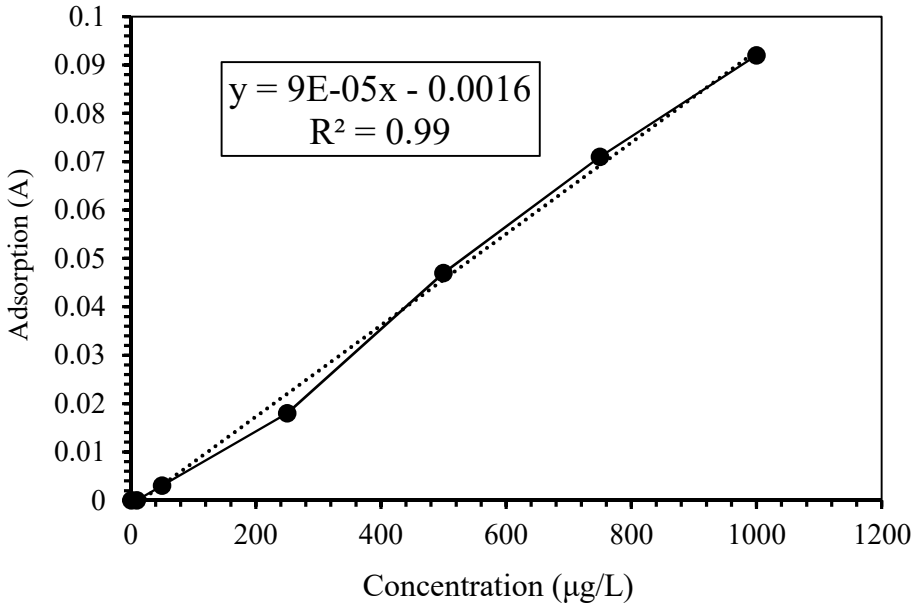

Figure 4.1.2: Calibration curve plotted from the concentration values of the mother stock solution (µg/L) against the measured adsorption values from the extracted supernatant

4.1.4 Trace elemental concentration and composition (including barium)

The trace elemental composition of the sediment core samples have been analysed for this study through a Laser Ablation ICP-MS by the Stellenbosch University's Central Analytical Facility following Eggins, (2003). The instrument is prepared, whereby an Excimer laser, with a resolution of 193nm from ASI, is connected to an Agilent 7700 ICP-MS to analyse the trace elements within single mineral grains. This is followed by an ablation technique within helium (He) gas, at a flow rate of 0.35L/min. Then argon (Ar) (0.9L/min) and Nitrogen (N) (0.004L/min) are introduced into the ICP plasma. The preparation of the sample involves the preparation of the fusion disk for the XRF analysis through an automated Claisse M4 Gas Fusion instrument and ultrapure Claisse Flux, which utilizes a ratio of 1:10 of sample to flux. Subsequently, the coarsely crushed and finer chips of the sample are mounted on a 2.4 cm round resin disk and polished for analysis. To analyse trace elements within a fusion, two spots

on the sample, each of 100µm area, are ablated using a frequency of 10Hz and fluency of ~6 J/ cm^2. To quantify the trace element concentrations, a NIST 610 glass standard (values from Jochum et al., 2011) is used. At the beginning of each sequence, a fusion control standard, from certified basaltic reference material (BCR-2, and BHVO-1, values from Jochum et al, 2016), is analysed in order to validate the effective ablation of fused material. In addition, two standards, BCR-2G and BHVO-2G, were analysed every 15 samples (values from GeoReM: Jochum et al 2005). The sample data is processed using Glitter v4.4.4 software (Access Macquarie Ltd., Macquarie University NSW 2109).

4.1.5 Trace element distribution in sedimentary particles (SEM imaging)

The sediment samples were analysed by a Zeiss EVO MA 15 Scanning Electron Microscope (SEM) instrument, through a quantitative energy dispersive (ED) and working distance (WD) technique at the Electron Microbeam Unit of Stellenbosch University's Central Analytical Facility. With the use of an Oxford Instruments® X-Max 20 mm^2 detector and Oxford INCA software, the trace elements of the sediment were quantified by an energy dispersive x-ray (EDX) analysis. The energy dispersive spectroscopy is only suitable for defining major elements of minerals at concentrations over 0.1 wt% for heavy elements, and over 0.01 wt% for light elements. A suite of trace elements was quantified by WDS analysis through an Oxford Instrument ® Wave Dispersive X-ray Spectrometer and an Oxford INCA software. The counting time for the Sr peak was 60 seconds on peak and 30 seconds on the background. The beam conditions were 20 KV and approximately 1.0 A, with a working distance of 8.5 mm and a specimen beam current of -20.00 nA, during the quantitative analyses (CAF lab, 2018). During mineral evaluation, the counting time was 10 seconds live-time. Natural mineral standards were used for standardization and verification of the analyses. The system is designed to perform high-resolution imaging concurrently with quantitative analysis, with errors ranging

from ± 0.6 to 0.01wt% on the major elements using EDS and ± 0.01 to 0.02wt% on the trace element using WDS (CAF lab, 2018). However, the image output quality was lower than expected and the Zeiss EVO instrument returned low resolution images, therefore the SEM analysis was continued by the use of the Merlin instrument for backscatter electron detector (BSD) imaging. The sediment samples were loaded in a Zeiss MERLIN Field Emission Scanning Electron Microscope at the Electron Microbeam Unit of Stellenbosch University's Central Analytical Facility. Prior to imaging, the samples were prepared by mounting on aluminium stubs with double sided carbon tape. The samples were then coated with a thin (~10 nm thick) layer of gold, using an Edwards S150A Gold Sputter Coater (CAF lab, 2018). A Zeiss 5-diode Back Scattered Electron (BSE) Detector (Zeiss NTS BSD) and Zeiss Smart SEM software were used to generate BSE images. The samples were chemically quantified by semi-quantitative Energy Dispersive X-Ray Spectrometry (EDS) using an Oxford Instruments® X-Max 20 mm^2 detector and Oxford Aztec software. Beam conditions during the quantitative analysis and backscattered electron image analysis on the Zeiss MERLIN were 20 kV accelerating voltage, 11 nA probe current, with a working distance of 9.5 mm (CAF lab, 2018). The counting time was 10 seconds live-time. Gold is automatically excluded from analysis due to sample coating with gold. For fully quantitative un-normalized analyses the sample must be flat and have a high polish and be larger than the beam diameter which is approximately 1.5 µm and have a z-depth value more than the penetration depth of the electron beam (between 1-5 µm) (CAF lab, 2018).

4.1.6 Excess barium

The excess barium content is calculated from the total barium concentration as the fraction of barium that is not related to terrigenous aluminosilicate material (1). The terrigenous barium portion is calculated (2) by multiplying the total aluminium concentration with the detrital ratio

(Ba/Al). The detrital ratio of barium to aluminium, for the determination of the terrigenous barium content (2) is obtained by utilizing crustal composition values from sedimentary rocks, with an established ratio of 0.0075 (Dymond, Suess and Lyle, 1992).

$$Ba_{excess} = Ba_{total} - Ba_{terrigenous} \quad (1)$$

$$Ba_{terrigenous} = Al_{total} \times \left({}^{Ba}/_{Al}\right)_{detrital} \quad (2)$$

4.1.7 Statistical analysis

Microsoft excel was used to run regression analysis, whereby the concentrations of total barium and excess barium (biogenic barium) were plotted against other productivity proxies (TOC and chlorins) and terrestrial input concentrations (Al). Correlations between two variables were established by the coefficient of determination (R^2) and significance established using the P-values. A threshold of ($P < 0.1$) was applied to determine statistically significant correlations. R^2 values in the (0.3 – 0.5) range were labelled 'weak' relationships, R^2 values in the (0.5 – 0.7) range were labelled 'moderate' relationships and the R^2 values > 0.7 were labelled 'strong' relationships. The null hypothesis assumed here is that there is no relationship between two variables (e.g. barium and TOC).Through the null hypothesis it is determined whether the results were due to random chance and therefore do not support the hypothesis tested or if there is a significant correlation. A significant correlation between barium and the productivity proxies, means that it is a good indicator for paleoproductivity.

4.2 Continental environment: Mfabeni peatland

4.2.1 Sample collection and preparation

The TOC and trace elemental data was obtained from Dr. Andrea Baker (Stellenbosch University, Department of Earth Sciences) as published in Baker et al., (2014), where an 810 cm deep sediment core (SL6), was extracted from the central and deepest region of the Mfabeni peatland (28.15021°S; 32.52508°E). The core was extracted by a Russian peat corer consisting of a 5 cm diameter and 50 cm long core chamber in June 2011. The core was logged and photographed in the field and later described and sectioned into 1–2 cm increments in the laboratory. All samples were weighed before freeze-drying, then again afterwards to calculate bulk density and porosity of each segment.

4.2.2 Core description

As recorded by Baker *et al.*, (2014), the SL6 core includes several sediment types (Figure 4.2.1). The basal section of the core (depth between 340–110 cm) composed of a black fined-grained amorphous peat with very few rootlets (Figure 4.2.1).This is overlaid by a layer (depth between 110–61 cm) of black fine-grained amorphous peat with extensive rootlets, and dark brown “fibrous” peat. The topmost core layer (depth between 61–0 cm) that is composed of fine grained black amorphous peat sediment. The peat sediment core displays an average bulk density of 0.24 g cm^{-3} for the linear sedimentation rate for stage 5 (340 – 0 cm) (Baker *et al*., 2014).

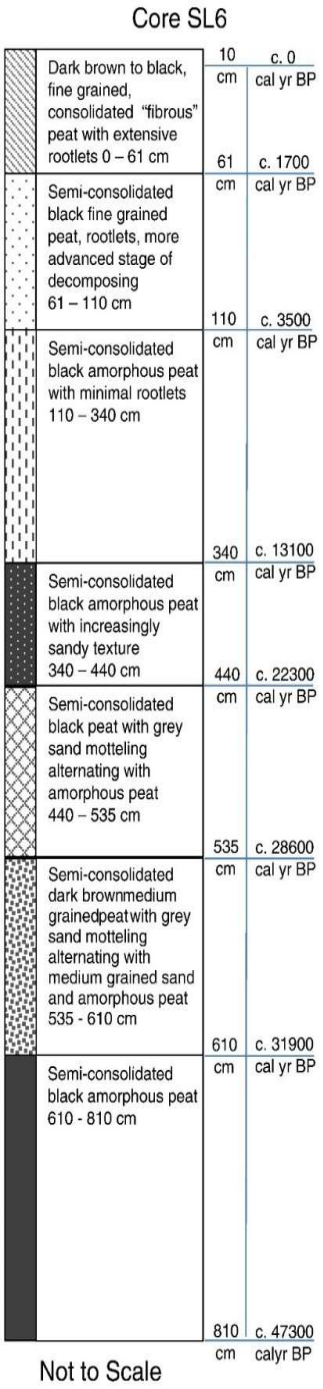

Figure 4.2.1: A stratigraphic representation of the SL6 core profile with the ages based on the calculated age model (modified from Baker et al., 2014)

4.2.3 Carbon and Nitrogen elemental analysis

The carbon and nitrogen analysis was conducted previously and published in Baker et al. (2014) and briefly reported here: Peat samples were combusted in a Thermo Scientific Flash 2000 organic elemental analyser, coupled to a Thermo Scientific Delta V Plus isotope ratio mass spectrometer via a Thermo Scientific Conflo IV gas control unit (detection limit 5 µg) at the Department of Archaeology, University of Cape Town. The sand samples, which contained a low C and N weight percentage, were combusted in a Thermo Finnigan Flash EA 1112 series elemental analyzer, coupled to a Thermo electron Delta Plus XP isotope ratio mass spectrometer via a Thermo Finnigan Conflo III gas control unit (detection limit 15 µg) (Baker et al., 2014). These data are used here as proxy for primary productivity.

4.2.4 Trace elemental concentration and composition, calculation of excess barium and statistical analysis

Detailed descriptions of the analyses has been provided in section 4.1.1 for trace element composition, in section 4.1.6 for excess barium calculation, and in section 4.1.7 for statistical analyses.

4.3 Coastal marine environment: offshore Namibia

4.3.1 Sample collection and preparation

The sample collection took place on the RV Mirabillus, organised by the regional research graduate network in oceanography as part of their summer school program, running from April 28th to May 24th 2019. Sample cores were collected from the Benguela upwelling system, from the North Namibian Cell (NNC; 20° S) and the Central Namibian Cell (CNC; 23°), located off-shore of the Namibian coast (Section 3.3.1, Figure 3.3.1). In each cell, two cores were sampled (see Figure 3.3.1 for cells and coring locations). Core were recovered by a multi-corer, where the sediment-water interface are collected. The cores were sectioned into 5cm intervals and samples were placed in plastic bags and transported back to the Stellenbosch University laboratory. The samples were processed and prepared by freeze-drying, and I further homogenized each sample by use of a mortar and pestle for the ICP-MS, XRF and chlorins analysis. For the SEM analysis, samples were placed within an epoxy resin solution, once the resin was oven dried, sample stubs were polished.

4.3.2 Core description

The bulk sediment composition consists of aluminosilicate materials, consisting of sand and mud rich laminated sediment. Sediment cores are dominated by diatomaceous rich muds which hold high contents of organic carbon, fish remains and some intervals of sea-shell fragments. Sediment cores ages where estimated by utilizing a sedimentation rate and age data applied by (Struck *et al.*, 2002), therefore 1cm intervals in the sediment cores (this study) represented 5.2 yrs. The sediment cores ranged from 0 – 20 cm and 0 – 15 cm depths, therefore they represent age ranges between 0 - 104 yrs, and this exhibits the modern environment in all four cores.

4.3.3 Chlorins, trace elements, SEM imaging, and statistical analysis

These analyses were described above (cf. section 4.1 Lake Baikal). The primary productivity of the Namibian coastal cores was examined using chlorin analysis (section 4.1.3). The composition and distribution of the trace metal contents of the samples core was analysed as described in section 4.1.4. The trace element distribution in sedimentary particles was analysed by the same SEM imaging method as the Lake Baikal core samples (section 4.1.5). The statistical analysis method applied was the same as in section 4.1.7.

Chapter 5: Results

As previously specified in Chapter 1, this study aims to determine the suitability of the application of barium, to reconstruct the productivity in a range of paleoenvironments. Paleoreconstructions that have utilized barium as a proxy have been documented in recent published literature (section 2.5). However, the vast majority of studies focused on the reconstruction of open/deep ocean environments. Thus this results in a knowledge gap relating to various other environments such as lacustrine and peatland. Here, the barium (Ba) profile in sediments was established in different environments and compared to other productivity (TOC and chlorophyll-a,) and environmental (C/N, Al and $\delta^{13}C$) proxies. This knowledge can then be used to assess whether barium might or cannot be used as paleoproductivity proxy in these environments.

5.1 Continental environment: Lake Baikal

The lacustrine barium (Ba) sediment profiles were constructed from a core retrieved from the Vydrino Shoulder located in the southern basin of Lake Baikal. The barium (Ba) concentration was then correlated with various other productivity proxies such as chlorophyll-a degradation products (this study) and TOC (from Mackay et al., 2014) and other paleo-environmental indicators such as C/N and $\delta^{13}C$ (from Mackay et al., 2014).

5.1.1 Depth profiles

The depth profiles of total Ba and excess Ba (Figure 5.1.1- Figure 5.1.4), TOC (Figure 5.1.1), C/N (Figure 5.1.2), chlorins (Figure 5.1.3) and $\delta^{13}C$ (Figure 5.1.4) exhibit different trends over the investigated Holocene period, 12-1 kyr ago. The total Ba concentration varied throughout the sediment depth profile, with an observed maximum (768 ppm) at 10.6 kyr ago and a minimum (621 ppm) at 2.7 kyr ago (Figure 5.1.1). The excess Ba profile displayed a

maximum (-593 ppm) at 10.6 kyr ago and a minimum (-326ppm) at 2.7kyr ago. The TOC and C/N similarly exhibit changes over the early and late-Holocene. The TOC profile exhibits a maximum (2.29 %) at 5.3 kyr ago and a minimum (1.21 %) at 10.3 kyr ago (figure 5.1.1), whereas the C/N ratio maximum (13) is displayed at 8.8 kyr ago and the minimum (10) at 7.3 kyr ago (Figure 5.1.2). The degradation products of chlorophyll-a (chlorins) fluctuate over varying time periods, with a maximum (1.27 µg/g) observed at 7.8 kyr ago and a minimum (0.25 µg/g) at 1.3 kyr ago (Figure 5.1.3). The $\delta^{13}C$ profile displays a maximum (-28.05‰) at 976 yr. ago and a minimum (-30.2‰) at 4.9 kyr ago (Figure 5.1.4).

5.1.2 Ba vs other paleoproductivity proxies

The statistical analysis of total Ba throughout the whole Holocene period does not show any correlation with TOC (P > 0.1,$R^2 = 0.01$) (Figure 5.1.1 b) or chlorins (P > 0.1,$R^2 = 0.13$) (Figure 5.1.3 b). However, there are periods within the Holocene, where the total Ba concentration profile shows a similar distribution to TOC (Figure 5.1.1 a) and chlorins (Figure 5.1.3 a) profiles. The total Ba vs TOC correlation (Figure 5.1.1 b) during the early Holocene (11 - 10 kyr ago) is moderately strong and positive ($R^2 = 0.63$), and no correlation was observed over the mid-Holocene (9.2 - 4.2kyr ago) and late Holocene (2.7 - 1 kyr ago) ($R^2 < 0.05$). The total Ba vs chlorin (Figure 5.1.3 b) correlation displays a similar relationship as total Ba vs TOC (Figure 5.1.1 b), whereby the correlation is positive and strong ($R^2 = 0.98$) in the Early-Holocene (11 - 9.5kyr ago), and becomes weaker ($R^2 = 0.20$) in the mid-Holocene (8 - 4 kyr ago), but is not statistically significant (P > 0.1). In the late-Holocene (2 - 1 kyr ago), the total Ba vs chlorin relationship is significant but weak (P= 0.009,$R^2 = 0.12$). None of these correlations are statistically significant (P > 0.1 for all Ba vs TOC correlations) partially due to the low number of samples in each time period, e.g. n=3 for the early Holocene, and can only serve as indications for potential correlations.

5.1.3 Excess Ba vs other paleoproductivity proxies

The statistical analysis of excess Ba throughout the whole Holocene period does not display a correlation with TOC (P < 0.1,$R^2 = 0.02$) (Figure 5.1.1 d) or chlorins (P > 0.1,$R^2 = 0.08$) (Figure 5.1.3 d). However, there are periods within the Holocene, where the excess Ba concentration profile shows a similar distribution to TOC (Figure 5.1.1 c) and chlorins (Figure 5.1.3 c) profiles. There is a moderately positive relationship between excess Ba vs TOC (Figure 5.1.1 d) over the early-Holocene (11 - 9 kyr ago) ($R^2 = 0.55$) and a significantly (P = 0.0004) strong negative ($R^2 = 0.70$) correlation over the mid-Holocene (9 - 6.8 kyr ago). No correlation is observed over the late-Holocene (2.1 - 1 kyr ago) ($R^2 = 0.009$) between excess barium and TOC. These correlations for the early and late-Holocene are not statistically significant (P > 0.1), due to the low number of samples in each section, e.g. n=3 for the early Holocene, and are only applied to display potential indicators for a relationship. No correlation is observed between the excess Ba vs chlorins (Figure 5.1.3 d) throughout the mid-Holocene ($R^2 = 0.01, 8.5 - 2$ kyr ago), with a moderate positive correlation in the early-Holocene ($R^2 = 0.49$, 10.5 - 8.5 kyr ago) and late-Holocene ($R^2 = 0.35, 1.3 - 1$ kyr ago). These excess Ba vs chlorins correlations throughout the Holocene are not statistically significant (P > 0.1).

5.1.4 Ba vs. environmental proxies

The relationship between total Ba and Al (Figure 5.1.5 c) throughout the Holocene is moderately positive and statistically significant (P =<0.001, $R^2 = 0.66$). It is significant and strong (P = 0.019, $R^2 = 0.99$) in the early-Holocene (12 - 10.3 kyr ago) (Figure 5.1.5 b). This relationship weakens, but continues to be positive ($R^2 = 0.47$) in the mid-Holocene (9 - 6.8 kyr ago). The total Ba vs Al relationship strengthens again ($R^2 = 0.95$) in the late-Holocene (3.3 - 1 kyr ago) but is not statistically significant (P = 0.19).

The total Ba vs C/N relationship (Figure 5.1.2 b) in the early Holocene (11.1-7.3 kyr ago) is weak and negative ($R^2 = 0.26$) and no correlation is observed ($R^2 = 0.01$) throughout the mid-Holocene (6.1-5.2 kyr ago). The relationship moderately strengthens ($R^2 = 0.57$) over the late-Holocene (4.9-1kyr ago) and becomes positive. Again, none of these correlations are statistically significant (P > 0.1) and can only serve as indications. A strong negative correlation is observed between total Ba concentration and $\delta^{13}C$ (Figure 5.1.4 b) over the early-Holocene (11-9.8 kyr ago) ($R^2 = 0.88$), which weakens and becomes positive over the mid-Holocene (9-6 kyr ago) ($R^2 = 0.26$) and then strengthens and becomes negative again over the late-Holocene (4.2-1 kyr ago) ($R^2 = 0.51$), however none of the correlations are statistically significant (P > 0.1).

5.1.5 Excess Ba vs environmental proxies

The relationship between excess Ba vs C/N (Figure 5.1.2 d) demonstrates similar trends as excess Ba vs TOC (Figure 5.1.1 d), whereby, there is a weak negative relationship between excess Ba and C/N over the early-Holocene (11.1-8.2 kyr ago) ($R^2 = 0.20$) and no correlation was observed over the mid-Holocene (8-4.2 kyr ago) ($R^2 = 0.09$). The late-Holocene (4.2-1 kyr ago) displays a strong negative correlation ($R^2 = 0.81$) between excess Ba and C/N. Again, the correlations of the mid and late-Holocene are not statistically significant (P > 0.1) and can only serve as indications, however the early-Holocene correlation is significant (P = 0.09). The relationship between excess Ba vs $\delta^{13}C$ (Figure 5.1.4 d) is negative and strong ($R^2 = 0.92$) in the early-Holocene (11-9 kyr ago), but no correlation was observed ($R^2 = 0.0004$) over the mid-Holocene (8.9-7 kyr ago). Over the late-Holocene (4.2-1 kyr ago) the relationship is weak and negative ($R^2 = 0.21$). Again, the correlations throughout the early-Holocene and late-Holocene are not statistically significant (P > 0.1).

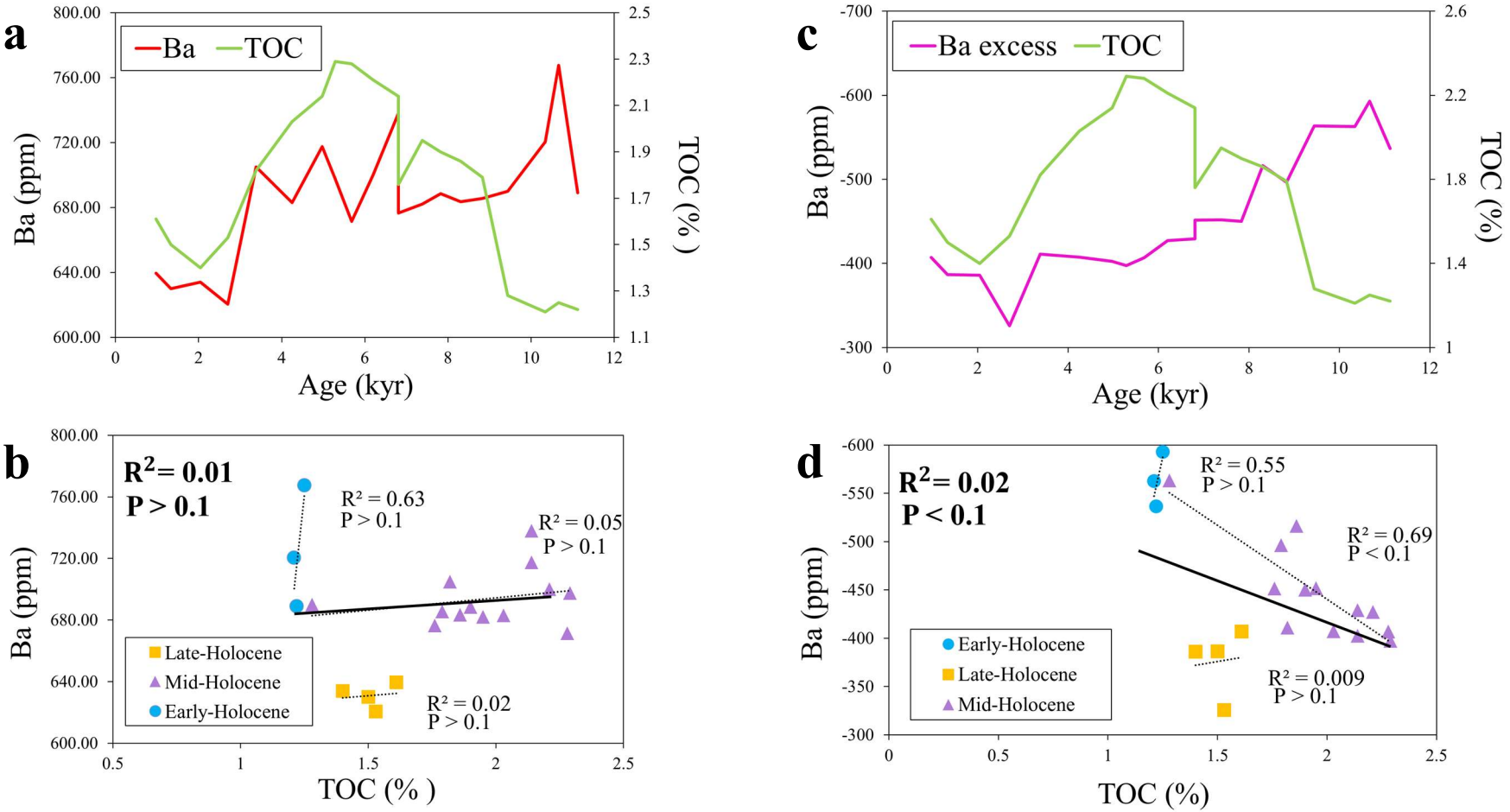

Figure 5.1.1 TOC and (a) total barium and (c) excess barium contents from 12000 to 1000 yrs ago in sediment core CON-605-5, South Basin, Lake Baikal, Russia. Regression lines in (b, d) are generated for the early-Holocene (12-10 kyr ago; blue), mid-Holocene (8.2-4.2 kyr ago; purple) and late-Holocene (4.0-1.0 kyr ago; yellow). The regression lines serve for visualisation and are not indicative of statistical significance. The reader is referred to the text for reports of statistical significance (i.e. p-values).

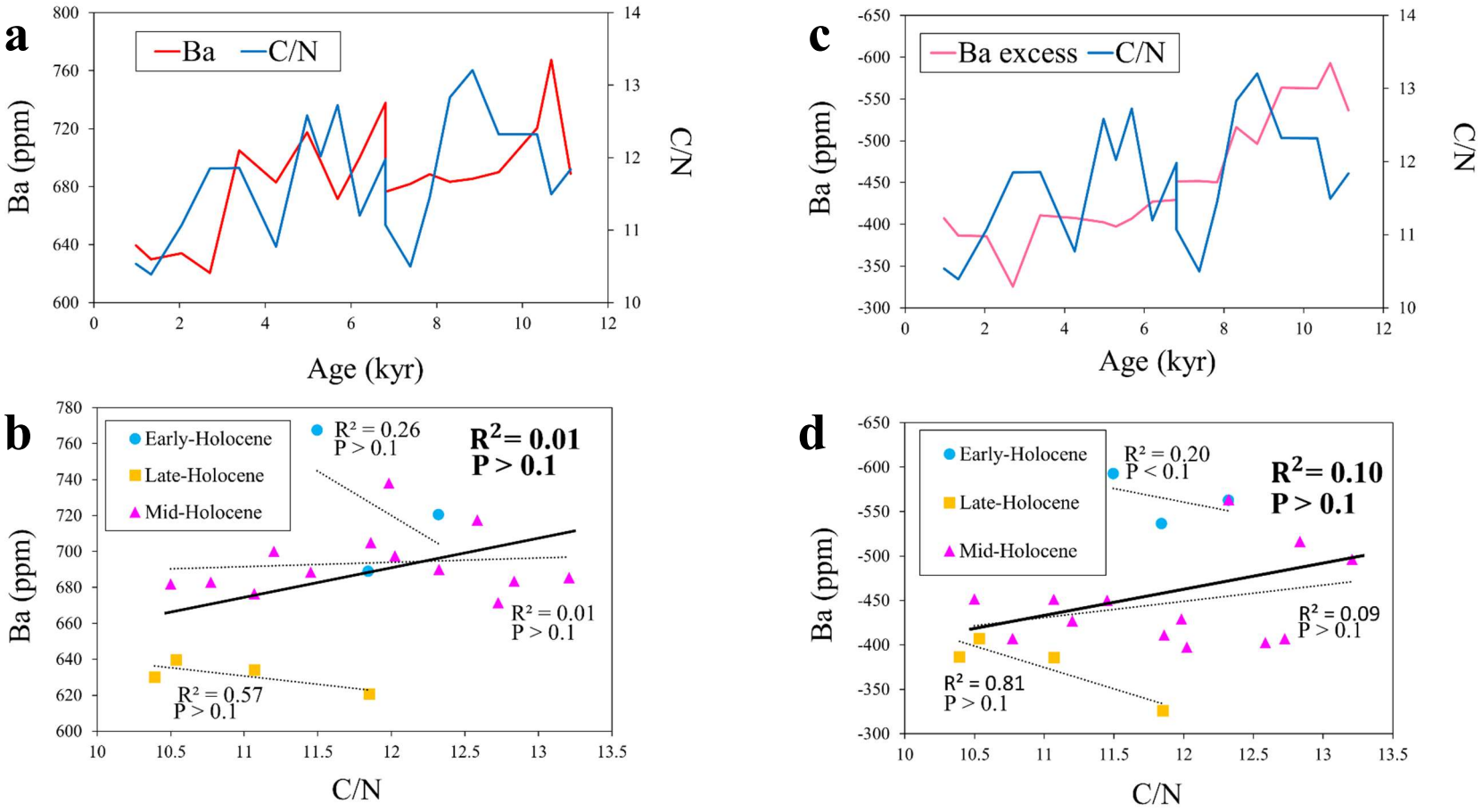

Figure 5.1.2 C/N and (a) total barium and (c) excess barium contents from 12000 to 1000 yrs ago in sediment core CON-605-5, South Basin, Lake Baikal, Russia. Regression lines in (b, d) are generated for the early-Holocene (12-10 kyr ago; blue), mid-Holocene (8.2-4.2 kyr ago; purple) and late-Holocene (4.0-1.0 kyr ago; yellow). The regression lines serve for visualisation and are not indicative of statistical significance. The reader is referred to the text for reports of statistical significance (i.e. p-values).

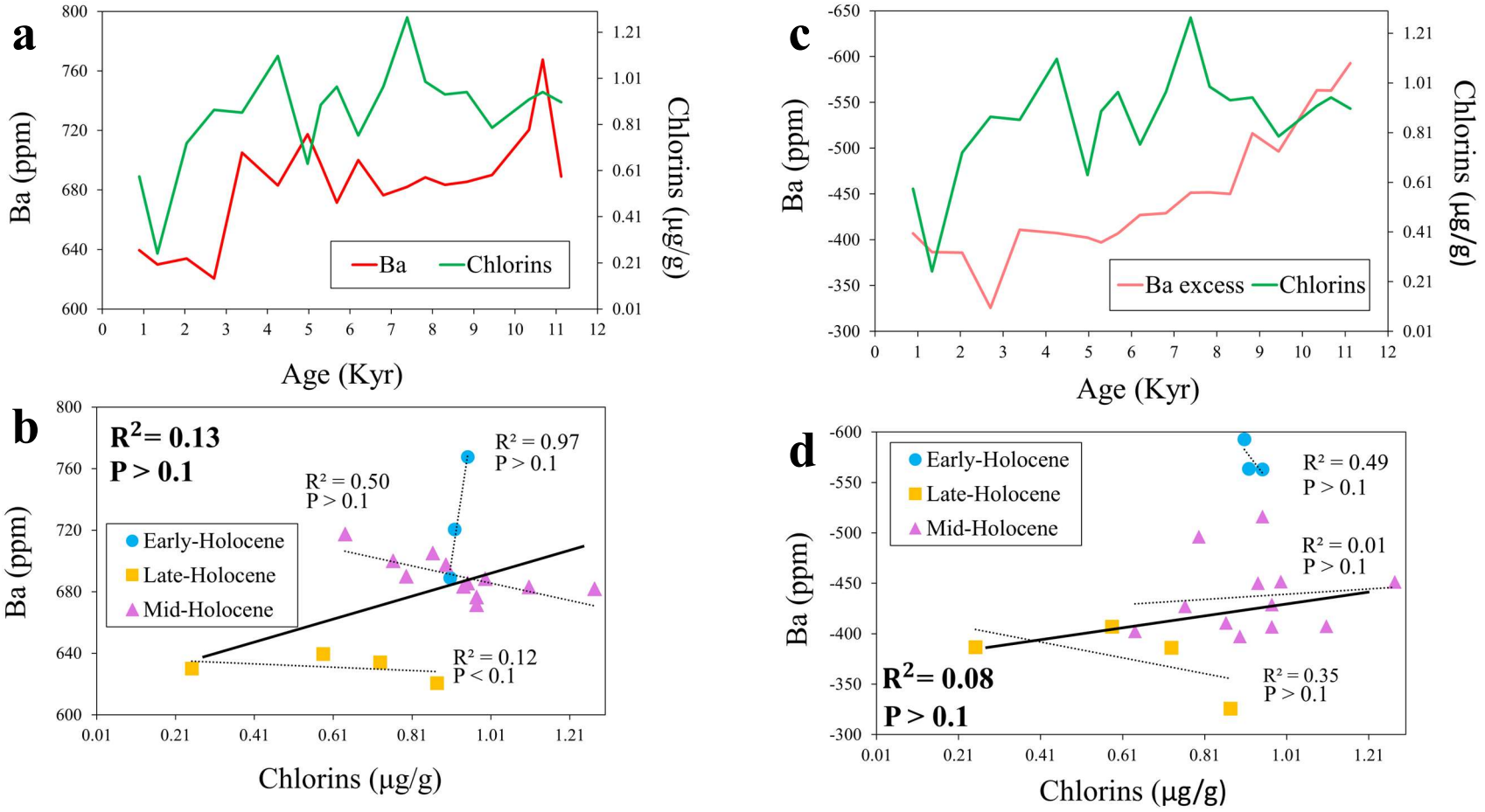

Figure 5.1.3 Chlorins and (a) total barium and (c) excess barium contents from 12000 to 1000 yrs ago in sediment core CON-605-5, South Basin, Lake Baikal, Russia. Regression lines in (b, d) are generated for the early-Holocene (12-10 kyr ago; blue), mid-Holocene (8.2-4.2 kyr ago; purple) and late-Holocene (4.0-1.0 kyr ago; yellow). The regression lines serve for visualisation and are not indicative of statistical significance. The reader is referred to the text for reports of statistical significance (i.e. p-values).

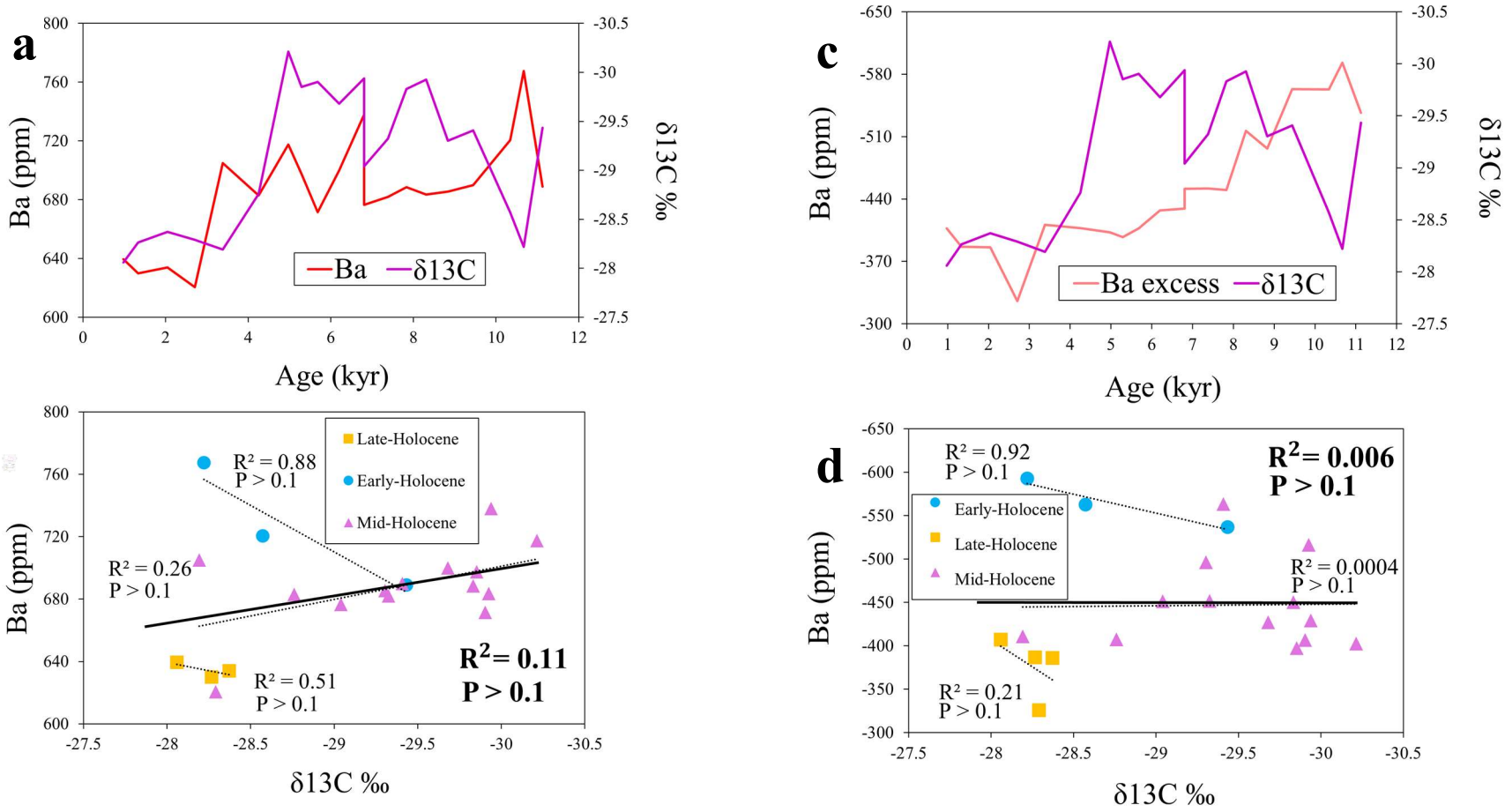

Figure 5.1.4 $\delta^{13}C$ and (a) total barium and (c) excess barium contents from 12000 to 1000 yrs ago in sediment core CON-605-5, South Basin, Lake Baikal, Russia. Regression lines in (b, d) are generated for the early-Holocene (12-10 kyr ago; blue), mid-Holocene (8.2-4.2 kyr ago; purple) and late-Holocene (4.0-1.0 kyr ago; yellow). The regression lines serve for visualisation and are not indicative of statistical significance. The reader is referred to the text for reports of statistical significance (i.e. p-value).

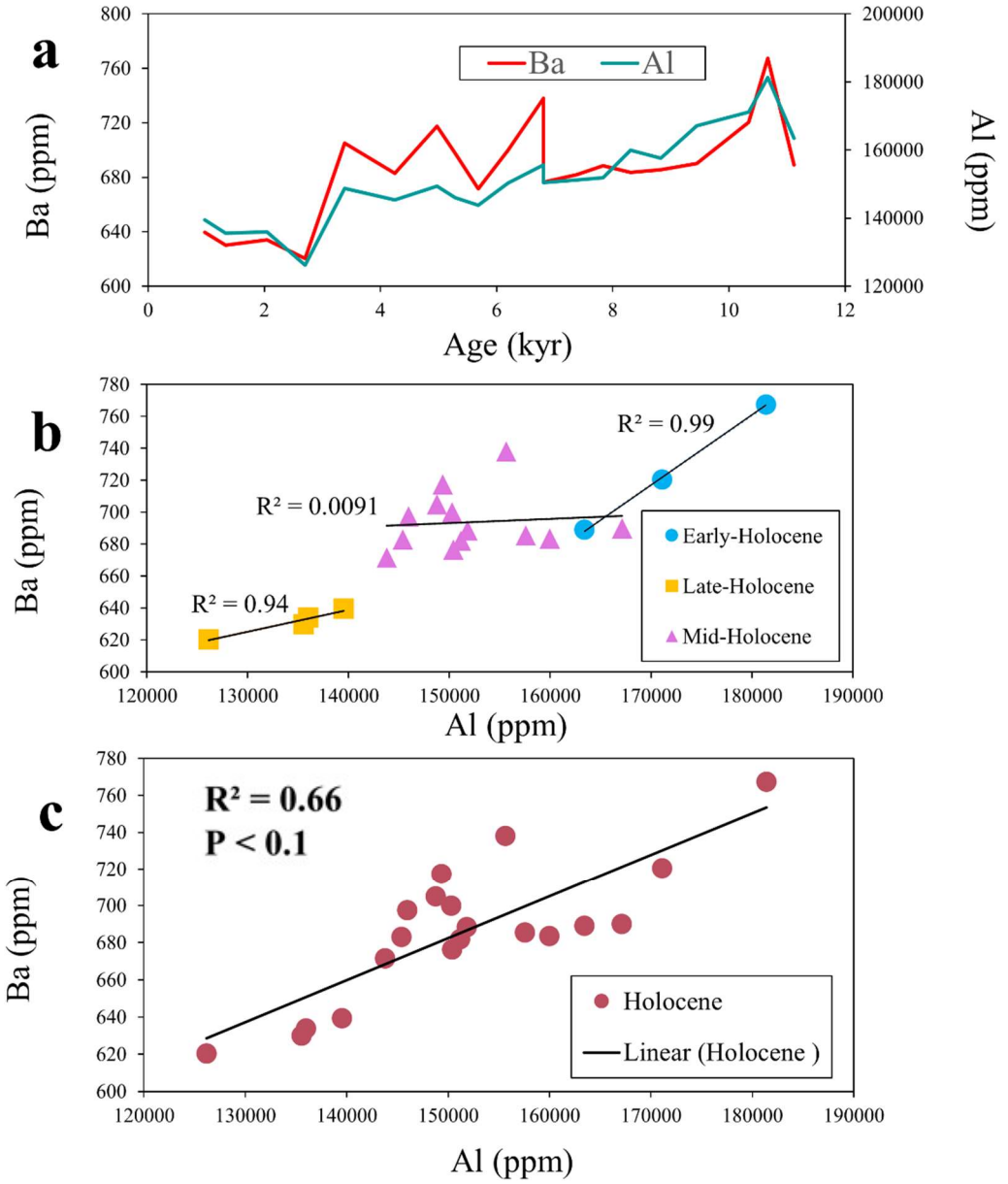

Figure 5.1.5: (a) Total barium and Al, from 12000 to 1000 yrs ago in sediment core CON-605-5, South Basin, Lake Baikal, Russia. Regression lines in (b) are generated for the early-Holocene (12-10 kyr ago; blue), mid-Holocene (8.2-4.2 kyr ago; purple) and late-Holocene (4.0-1.0 kyr ago; yellow). Regression line in (c) generated for the Holocene (early to late; 12 – 1.0 kyr ago). The regression lines serve for visualisation and are not indicative of statistical significance. The reader is referred to the text for reports of statistical significance (i.e. p-values).

5.1.5 SEM imaging

The Lake Baikal sediment core (CON01-605-5) (Figure 5.1.6) has been analysed by scanning electron microscopy (SEM) to determine the sediment composition and morphology. Samples analysed were located in upper core (0 – 52 cm). Using the 'Bacon' Age-depth model applied by Mackay *et al*., (2017), the samples analysed have been dated (0 - 2 kyr ago). As recorded by Stavreva, (2018) the bulk mineral composition consists of majority quartz, feldspars, amphibole, pyroxene and clays. The abundance of clastic to biological material fluctuated throughout the core depth, however, the sediment is clearly dominated by various diatom species. Diatoms concentrated in the upper-most interval of the sediment profile (0 – 12 cm), and gradually decreased down core (Figure 5.1.6).

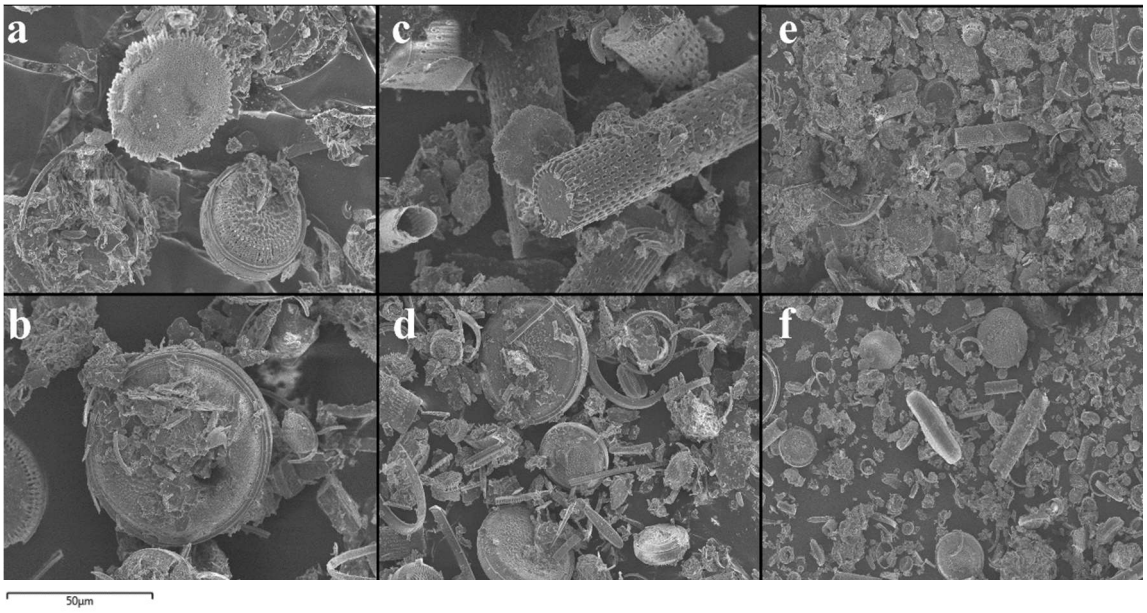

Figure 5.1.6: False colour SEM image; 0-12 cm core depth (a and b), 20-32 cm core depth (c and d) and 40-52 cm core depth (e and f).

False colour elemental maps (Figure 5.1.7) were created for sediment core depths 0-12cm, 20-32 cm and 40-52 cm. The elements analysed included aluminium (Al), barium (Ba) and silica (Si), where Al represents the lithogenic portion of the sediment and the Si represents the opal shells of diatoms and therefore the biogenic portion of the sediment. SEM images were analysed in order to determine whether barium is precipitated by biological organisms such as phytoplankton, or whether it chemically precipitates and forms minerals such as barite in the different aquatic environments. In the case of Lake Baikal, throughout the sediment core, barium has not been detected by the SEM analysis applied (Figure 5.1.7).

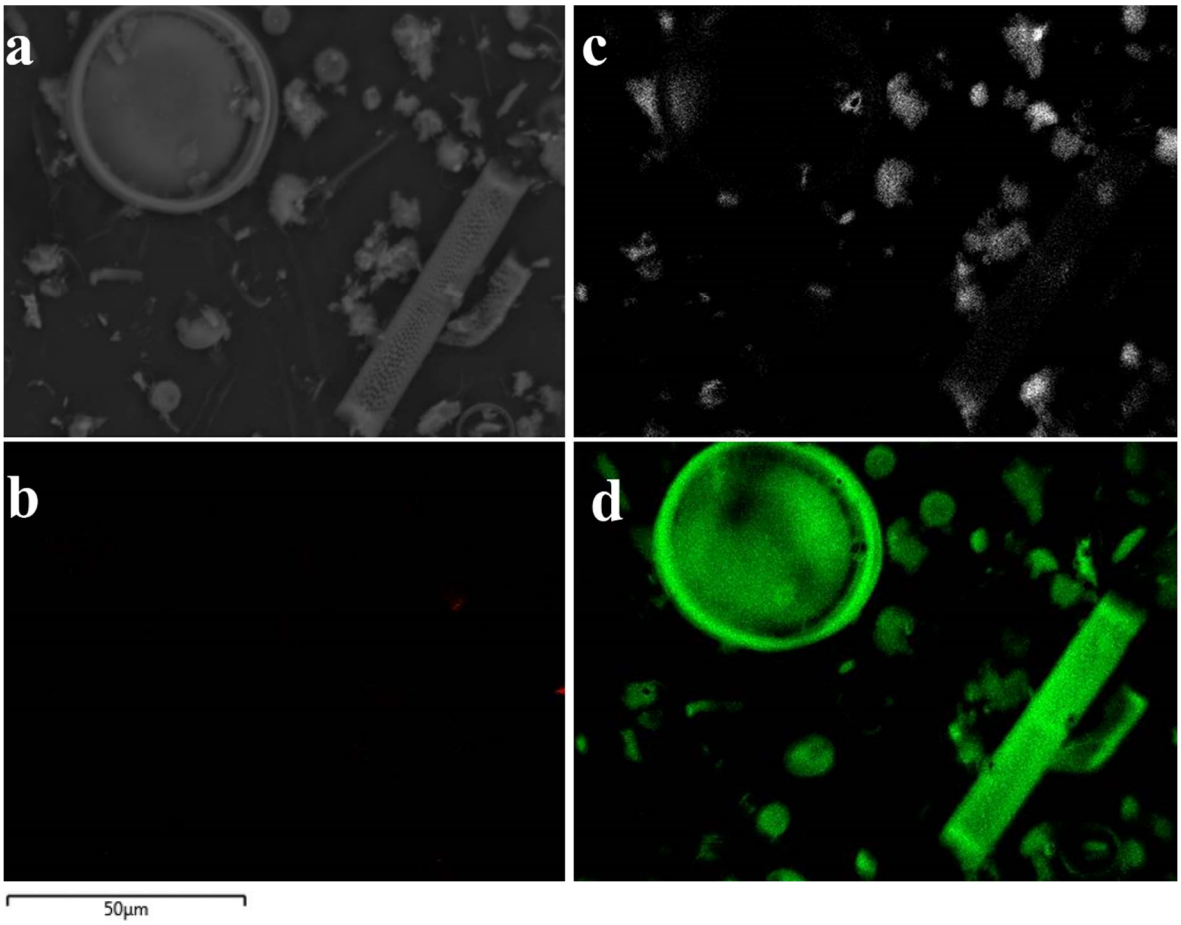

Figure 5.1.7: Elemental maps obtained via SEM -EDX; (a) original image, (b) barium, (c) Al, and (d) Si

5.2 Continental environment: Mfabeni peatland

Sedimentary Ba profiles were constructed over 12 kyr, spanning from the last glacial maximum, into the late Holocene, in the Mfabeni peat located in northern region of the Kwazulu-Natal province, South Africa. The Ba concentration was correlated with other paleoreconstruction proxies such as TOC and Al concentration as indicator of lithogenic input. The TOC concentrations were previously published in (Baker et al. 2014).

5.2.1 Depth profiles

The depth profiles of total Ba, excess Ba, TOC and Al display opposing trends that span from the early Holocene (14 kyr ago) to present day. The total Ba concentration varied throughout the sediment depth profile (Figure 5.2.1a), displaying a maximum (501 ppm) at 7.1 kyr ago and a minimum (40.2 ppm) at 3.4 kyr ago. (Figure 5.2.1 c) shows the calculated excess Ba that exhibits changes in concentration over time, with Ba excess concentration maximum (227 ppm) at 6.4 kyr ago and a minimum (-70 ppm) at present day. The TOC (Figure 5.2.1 a) and Al (Figure 5.2.2 a) profiles both exhibit fluctuations over the Holocene (14kyr to 2kyr) and into the modern environment (2kyr to present day). There is a minimum (19 %) TOC (Figure 5.2.1 a) at 7.1 kyr ago, which increases to a maximum (52%) at 3.4 kyr ago. The Al concentration (Figure 5.2.2 a) displays a minimum concentration (4995 ppm) at the early Holocene of 12.7 kyr ago, which increases over the late Holocene, 2.2 kyr ago, to a maximum (44134 ppm).

5.2.2 Ba vs other paleoproductivity proxies

The statistical analysis of total Ba throughout the whole Holocene period does not show any correlation with TOC (P > 0.1,$R^2 = 0.09$) (Figure 5.2.1 b), However, there are periods within the Holocene, where the total Ba concentration profile shows a similar distribution to TOC (Figure 5.2.1 a). The total Ba vs TOC relationship (Figure 5.2.1 a) is strong ($R^2 = 0.92$) and negative over the early Holocene (12 - 9 kyr ago), however the negative trend weakens throughout the mid-Holocene (8 - 5.8 kyr ago) to ($R^2 = 0.32$). These correlations are not statistically significant though (P >0.1). No correlation is indicated ($R^2 = 0.002$) over the late Holocene (4.5-2.2 kyr ago) and only faintly strengthens over the modern environment (2.2 kyr ago to present day) to a weak negative ($R^2 = 0.13$), but not significant (P> 0.1) relationship. None of these correlations are statistically significant partially due to the low number of samples in each time period and can only serve as indications for potential correlations.

5.2.3 Excess Ba vs other paleoproductivity proxies

The statistical analysis of excess Ba throughout the whole Holocene period does not show any correlation with TOC (P > 0.1,$R^2 = 0.01$) (Figure 5.2.1 d). The excess Ba vs TOC graph (Figure 5.2.1 c) exhibits a similar trend to the total Ba vs TOC relationship (Figure 5.2.1 c), as it displays a strong negative, but not statistically significant correlation ($P = 0.20$, $R^2 = 0.90$) in the early Holocene (12-9.8 kyr ago). This trend becomes weak and negative ($P = 0.24$, $R^2 = 0.26$) over the mid-Holocene (8.5-6 kyr ago). There is no correlation between excess Ba vs TOC through the late Holocene (4.2-2.3 kyr ago) ($P = 0.95$, $R^2 = 0.005$) and through the modern environment (2.2 kyr ago to present day) ($P = 0.79$, $R^2 = 0.04$). None of

these correlations are statistically significant partially due to the low number of samples in each time period and can only serve as indications for potential correlations

5.2.4 Ba vs. Al as proxy of lithogenic material

The total Ba vs Al correlation (Figure 5.2.2 c) is moderately positive and statistically significant throughout the Holocene record and modern environment ($P < 0.1, R^2 = 0.75$). The relationship (Figure 5.2.2 b) is significant and strong ($P = 0.01$, $R^2 = 0.99$) in the early Holocene (12 - 10 kyr ago). This relationship weakens, but continues to be a significant correlation ($P = 0.05$, $R^2 = 0.47$) in the mid-Holocene (9 - 6.8 kyr ago). The total Ba vs Al relationship remains strong, but not statistically significant in the late Holocene (6 - 4 kyr ago) ($P = 0.14$, $R^2 = 0.94$) and the modern environment (3.9 kyr ago to present day) ($P = 0.18, R^2 = 0.90$).

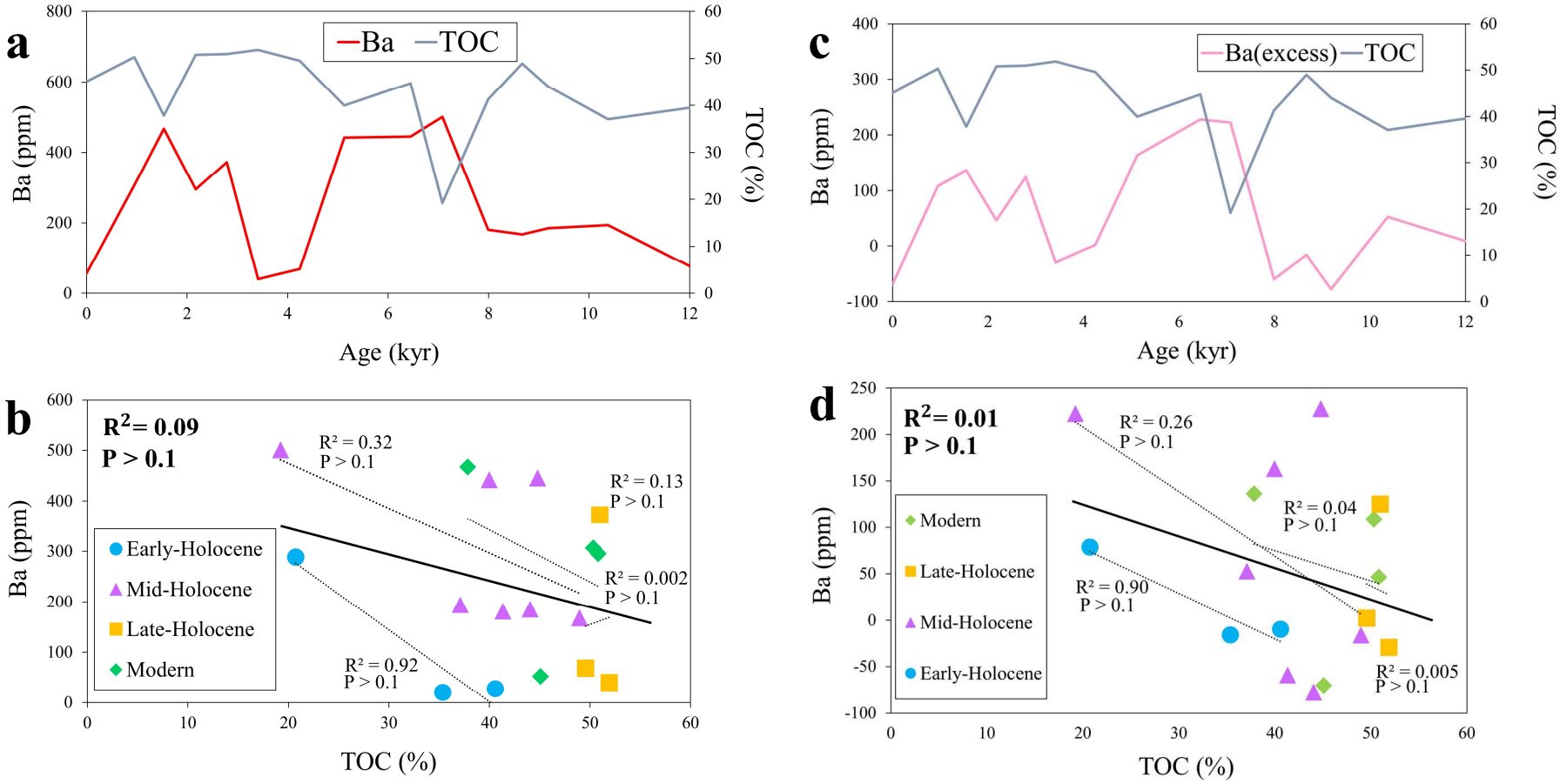

Figure 5.2.1: TOC and (a) total barium and (c) Excess barium over 12kyr from 12000 yrs ago to present day in sediment core SL6, Mfabeni peatland, South Africa. Regression lines in (b, d) are generated for the early-Holocene (12-10 kyr ago; blue), mid-Holocene (8.2-4.2 kyr ago; purple) and late-Holocene (4.0-1.0 kyr ago; yellow) and modern environment (2.2 – 0 Kyr ago; green). The regression lines serve for visualisation and are not indicative of statistical significance. The reader is referred to the text for reports of statistical significance (i.e. p-values).

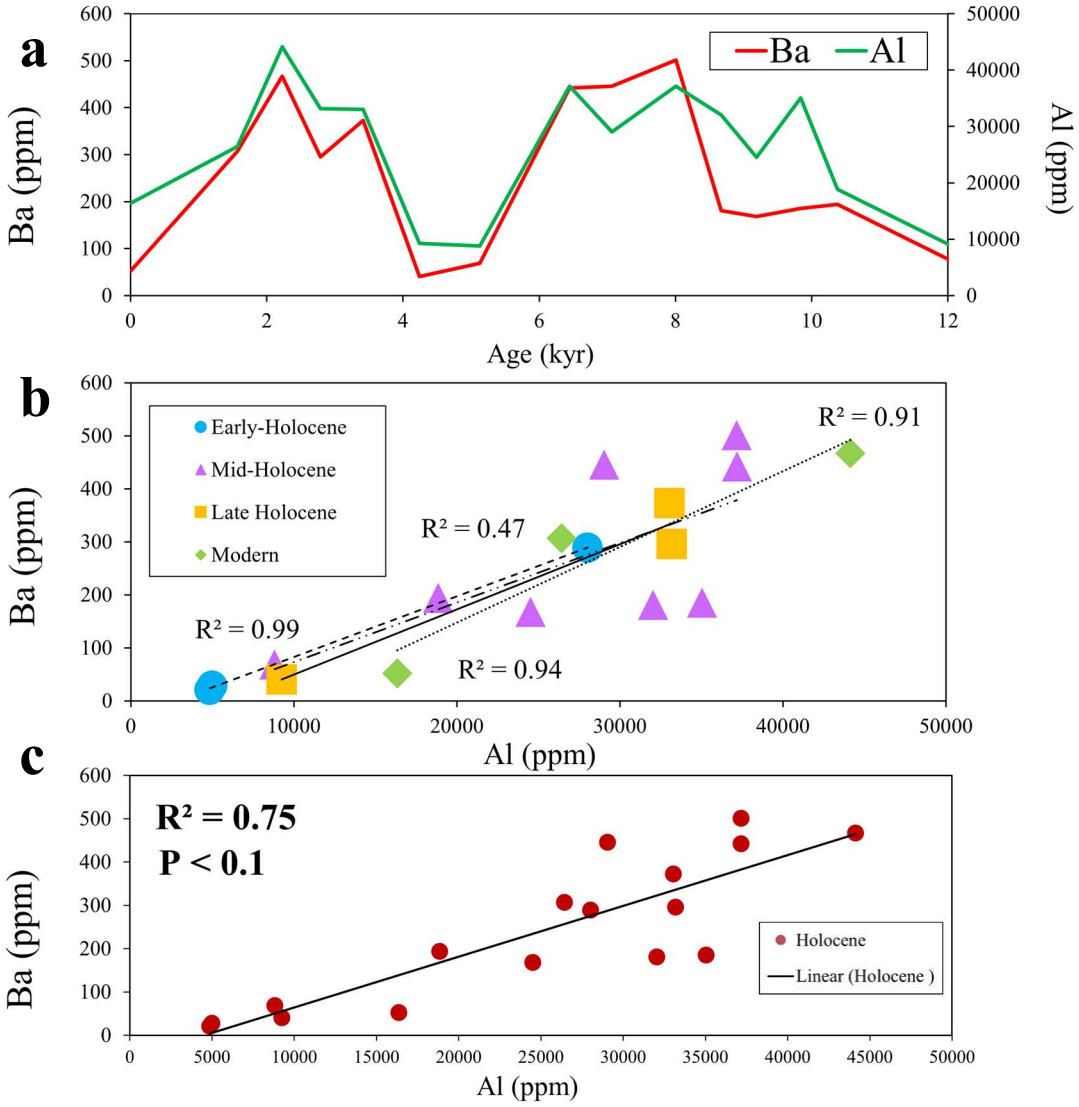

Figure 5.2.2: (a) Total barium and Al concentration over 12kyr from 12000 yrs ago to present day in sediment core SL6, Mfabeni peatland, South Africa. Regression lines in (b) are generated for the early-Holocene (12-10 kyr ago; blue), mid-Holocene (8.2-4.2 kyr ago; purple) and late-Holocene (4.0-1.0 kyr ago; yellow) and modern environment (2.2 – 0 Kyr; green). Regression line in (c) generated for the Holocene (early to late; 12 – 1.0 kyr ago) and modern (1.0 kyr to present). The regression lines serve for visualisation and are not indicative of statistical significance. The reader is referred to the text for reports of statistical significance (i.e. p-values).

5.3 Coastal marine environment: offshore Namibia

The coastal marine Ba sediment profiles were constructed from cores retrieved from the Benguela upwelling system, from the North Namibian Cell (NNC; 20° S) and the Central Namibian Cell (CNC; 23°). In each cell, two cores were sampled (see Figure 3.3.1 and Table 5.3.1 for cells and coring locations). Because cores from the same cells showed different Ba (and other proxies) depth profiles, results from both cores in both cells (i.e. of all four cores) are reported here. The Ba concentrations in all four cores were correlated with a paleoproductivity proxy such as chlorophyll-a degradation products and Al, as indicator of lithogenic input. The calculated ages for these cores range from c. 0 to 104 yrs (section 4.3.2).

Table 5.3.1: Sediment cores collected along the Benguela upwelling system. Cores (1 and 2) collected at the North Namibian cell (~20°S) *and cores (3 and 4) collected at the Central Namibian Cell* (~23°S).

Core 1	North Cell	20° 02 S	12° 59 E
Core 2	North Cell	20° 30 S	12° 03 E
Core 3	Central Cell	23° 02 S	14° 22 E
Core 4	Central Cell	23° 20 S	14° 02 E

5.3.1 Depth profiles

The depth profiles of total Ba (Figure 5.3.1, Figure 5.3.3), excess Ba (Figure 5.3.2), Al (Figure 5.3.3) and chlorins (Figure 5.3.1, Figure 5.3.2) extend over the modern environment. Within the North Namibian Cell (Figure 5.3.1), the Ba concentration varied throughout the sediment profiles, with observed maximums within the upper 5 cm (323 ppm at ~20°02 S and

of 136 ppm at ~20°30 S). Within the Central Namibian Cell (Figure 5.3.1), exhibited Ba maximums of (140 ppm) at 10-15 cm at ~23°02 S and (269 ppm) at 15-20 cm at ~23°20 S.

Variations of excess Ba concentration have also been recorded throughout in all four cores. In the North Namibian Cell (Figure 5.3.2) both cores exhibited several peak concentrations in excess Ba, e.g. (-70 ppm) at 15-20 cm at ~20°02 S and (11 ppm) at 10-15 cm at ~20°30 S. In the Central Namibian Cell (Figure 5.3.2) both cores also displayed several excess Ba concentration maximums, e.g. (12 ppm) at 10-15 cm at ~23°02 S and (195 ppm) at 15-20 cm at ~23°20 E.

Chlorins maximum concentrations in the North Namibian Cell (Figure 5.3.1) can be observe, such as (12.8 µg/g) at 15-20cm at ~20°02 S and (9.91 µg/g) at 0-5 cm at ~20°30 S. The chlorins concentration maximums in the Central Namibian Cell (Figure 5.3.1) are noted at 5-10 cm at ~23°02 S (30.2 µg/g) and at 15-20 cm at ~23°20 S (33.2 µg/g).

The Al concentration maximums in the North Namibian Cell (Figure 5.3.3) were recorded at 15-20 cm at ~20°02 S (44931 ppm) and at 0-5 cm at ~20°30 S (17464 ppm). Maximum concentrations of Al on in the Central Namibian Cell (Figure 5.3.3) can be observed at 10-15 cm (17146 ppm) at ~23°02 S and 15-20 cm at ~23°20 S (9843 ppm).

5.3.2 Ba vs other paleoproductivity proxies

In the North Namibian Cell the total Ba vs chlorins relationship of core 1 (20°02 S) is significant, strong (P = 0.076, $R^2 = 0.96$) and negative (Figure 5.3.1). The relationship between total Ba vs chlorins in core 2 (20°30 S) is significant, strong and positive (P = $0.077, R^2 = 0.98$) (Figure 5.3.1). In the Central Namibian Cell the total Ba vs chlorins relationship of core 3 (23°02 S) (Figure 5.3.1), is moderate, not significant (P = 0.5, R^2 =

0.48) and positive over the 5-10 cm depth range. A similar moderate, not significant ($P = 0.27$, $R^2 = 0.52$) yet negative trend is observed in core 4 (23°20 S) (Figure 5.3.1).

5.3.3 Ba excess vs other paleoproductivity proxies

In the North Namibian Cell, the excess Ba vs chlorins correlation of core 1 (20°02 S) (Figure 5.3.2) is significant, strong ($P = 0.03$, $R^2 = 0.93$) and positive. This relationship in core 2 (20°30 S) (Figure 5.3.2) is drastically lower, not significant ($P = 0.87$, $R^2 = 0.03$) and becomes negative below 5-10 cm. In the Central Namibian Cell (Figure 5.3.2), the excess Ba vs chlorins trend of core 3 (23°02 S) is moderate ($P = 0.50$, $R^2 = 0.48$) with a positive trend from present day to 5-10 cm. The relationship in core 4 (23°20 S) is a moderate, not significant and negative correlation ($P = 0.27$, $R^2 = 0.51$) from 10-15 cm depth to present day (Figure 5.3.2).

5.3.4 Ba vs Al as proxy of lithogenic material

In the North Namibian Cell (Figure 5.3.3), the relationship of total Ba vs Al of core 1 (20°02 S) is weak and positive ($P = 0.5$, $R^2 = 0.25$) from present day down to 10-20cm depth. The correlation of the total Ba vs Al relationship in core 2 (20°30 S) is strong and positive yet not significant ($P = 0.19$, $R^2 = 0.90$) (Figure 5.3.3). In the Central Namibian Cell (Figure 5.3.3), the total Ba vs Al correlation of core 3 (23°02 S) is significant, strong ($P = 0.0003$, $R^2 = 0.99$) with a positive trend. A similar positive and significant trend ($P = 0.03$, $R^2 = 0.93$). is observed for core 4 (23°20 S) (Figure 5.3.3).

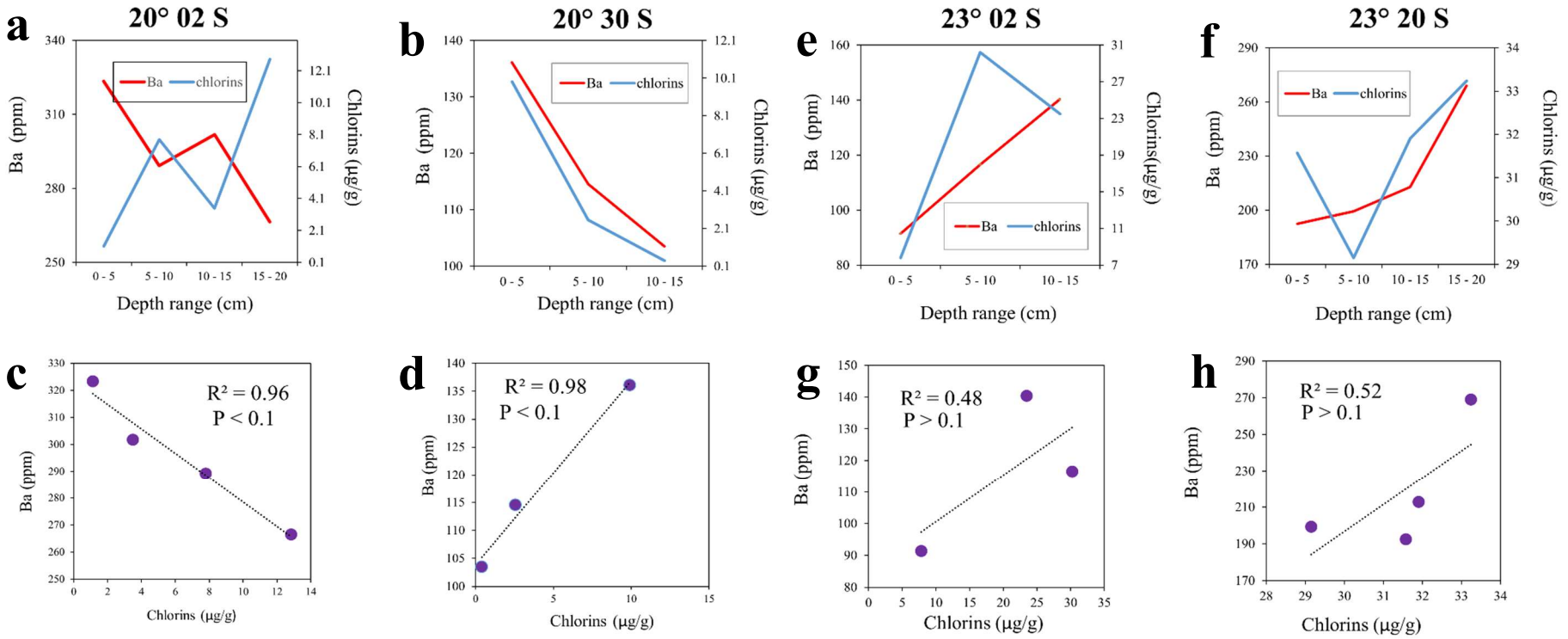

Figure 5.3.1: Total barium and chlorins concentration in sediment cores of the North Namibian cell (core 1 (a) 20°02 E and core 2 (b) 20°30 E) and the Central Namibian Cell (core 3 (e) 23°02 S and core 4 (f) 23°30 S); Total barium vs. chlorins content; where regression lines are generated for cores (1(c), 2(d), 3(g) an 4 (h)). The regression lines serve for visualisation and are not indicative of statistical significance. The reader is referred to the text for reports of statistical significance (i.e. p-values).

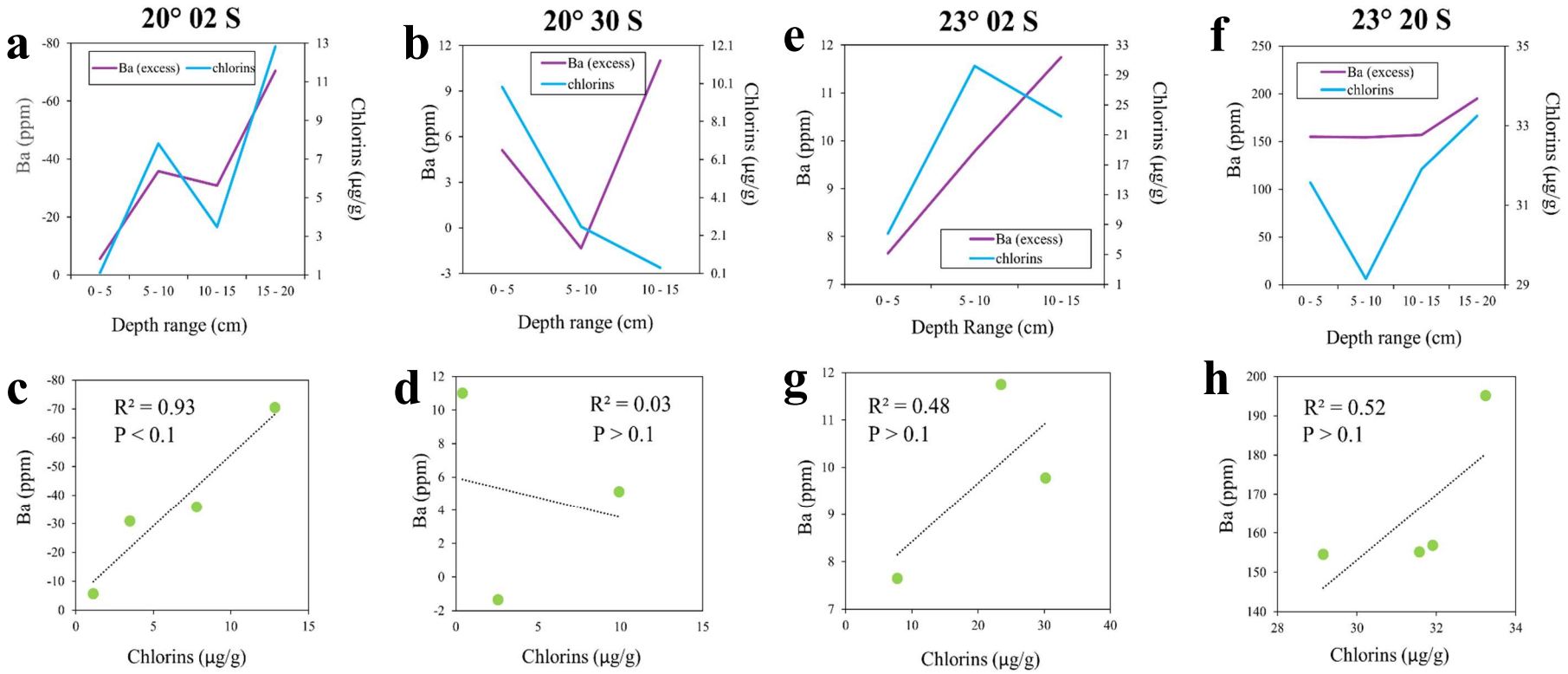

Figure 5.3.2: Excess barium and chlorins concentration in sediment cores of the North Namibian cell (core 1 (a) 20°02 E and core 2 (b) 20°30 E) and the Central Namibian Cell (core 3 (e) 23°02 S and core 4 (f) 23°30 S); Excess barium vs. chlorins content; where regression lines are generated for cores (1(c), 2(d), 3(g) an 4 (h)). The regression lines serve for visualisation and are not indicative of statistical significance. The reader is referred to the text for reports of statistical significance (i.e. p-values).

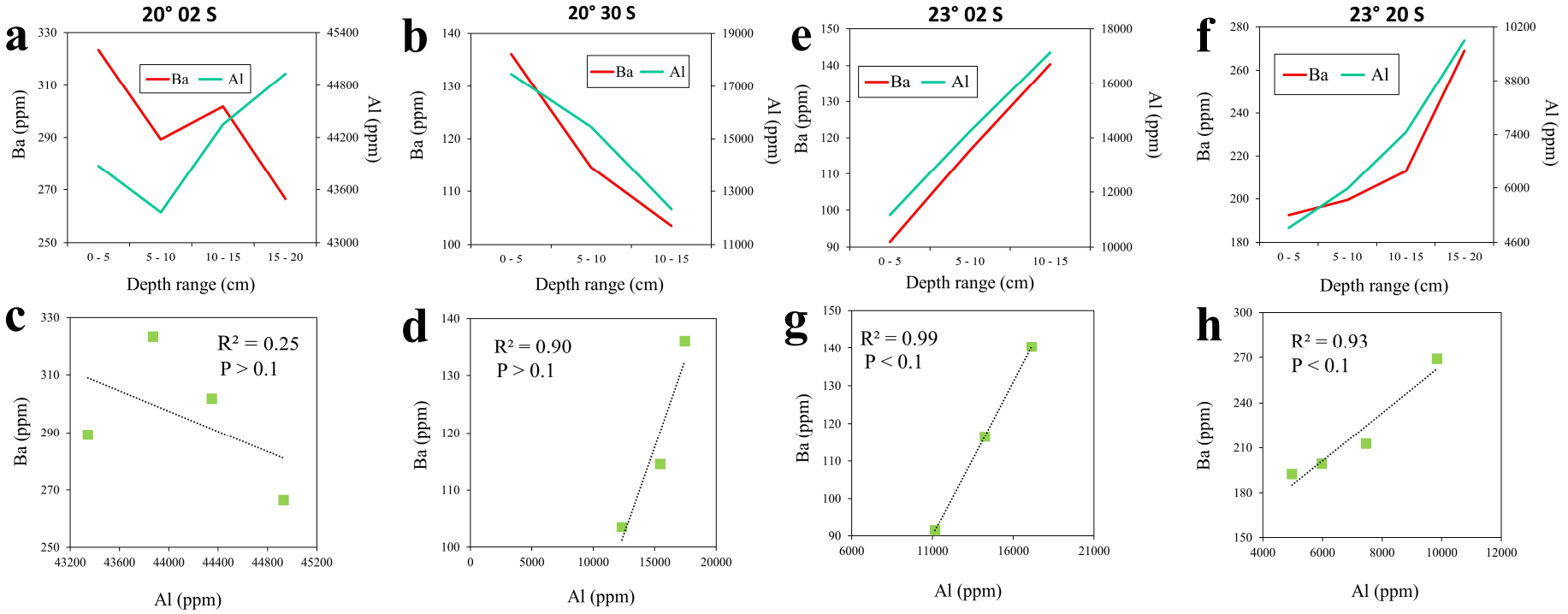

Figure 5.3.3: Total barium and Al concentration in sediment cores of the North Namibian cell (core 1 (a) 20°02 E and core 2 (b) 20°30 E) and the Central Namibian Cell (core 3 (e) 23°02 E and core 4 (f) 23°30 E); Total barium vs. chlorins content; where regression lines are generated for cores (1(c), 2(d), 3(g) an 4 (h)). The regression lines serve for visualisation and are not indicative of statistical significance. The reader is referred to the text for reports of statistical significance (i.e. p-values).

5.3.5 SEM imaging

Scanning electron microscopy (SEM) has been utilized to determine the sediment composition and morphology of the sediments cores of the North Namibian Cell (NNC; 20° S) and the Central Namibian Cell (CNC; 23°). The mid- section (5 -10 cm) section of sediment core 2 (20°30 S) and the top section (0 – 5cm) of sediment core 4 (23˚ 20 S) were analysed. Using the sedimentation rate applied by (Emeis *et al.*, 2009), the samples analysed have been dated to represent (0 - 104 yrs ago). The bulk sediment composition consists of majority aluminosilicate materials such as muds and clays. The abundance of clastic to biological material only displayed minor variation throughout the core depths, as both cores (2 and 4) exhibited dominant compositions of various diatom species.

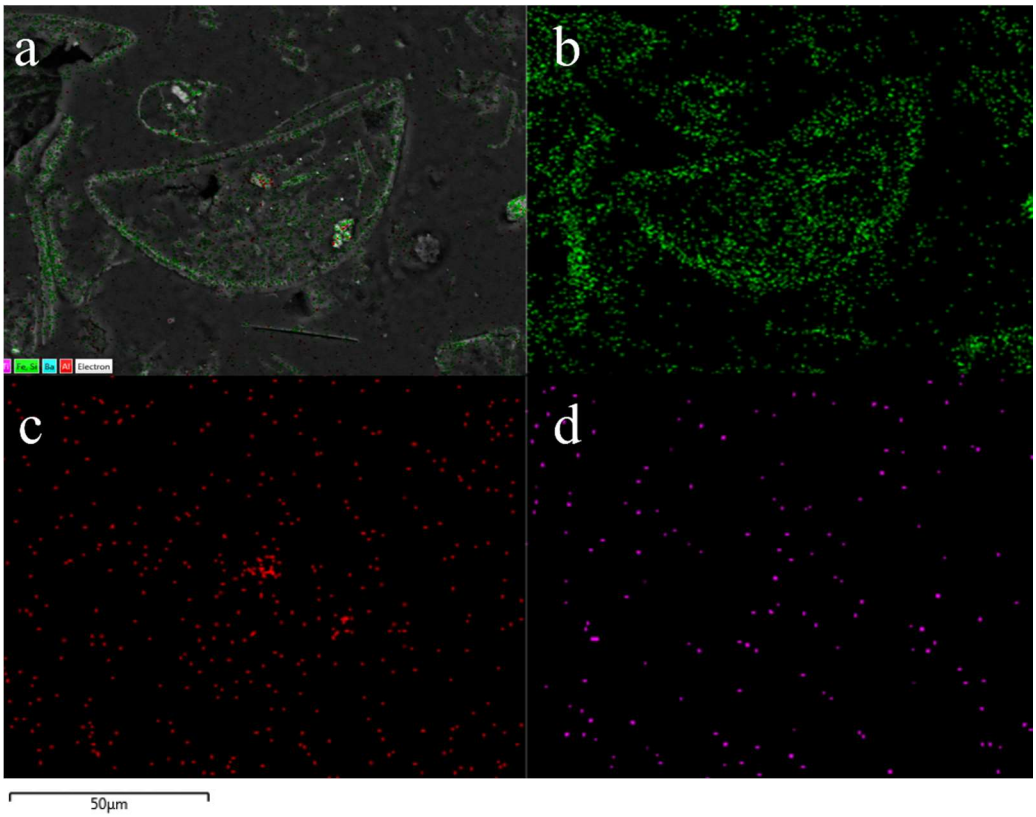

Figure 5.3.4: False colour elemental SEM map of sediment core 2 (5 - 10 cm depth); (a) original image, (b) Si, (c) Al, (d) Ba

False colour elemental maps were constructed for sediments cores (2 and 4), the elements analysed included aluminium (Al), barium (Ba), titanium (Ti) and silica (Si). SEM images were analysed in order to determine whether barium is precipitated by biological organisms such as phytoplankton, or whether it chemically precipitates and forms minerals such as barite in the different aquatic environments. For the North Namibian upwelling cell, sediment core 2 (Figure 5.3.4) displayed some barium associated with the aluminosilicate and biological fraction of the sediment. Therefore barium displays a broad precipitation pattern, and it is unclear to comment on whether it chemically or biologically precipitates in the North Namibian cell. However, sediment core 4 (Figure 5.3.5) of the Central Namibian upwelling region, displayed barium associated with only the aluminosilicate fraction of the sediment. Therefore, in the Central Namibian cell barium precipitates chemically.

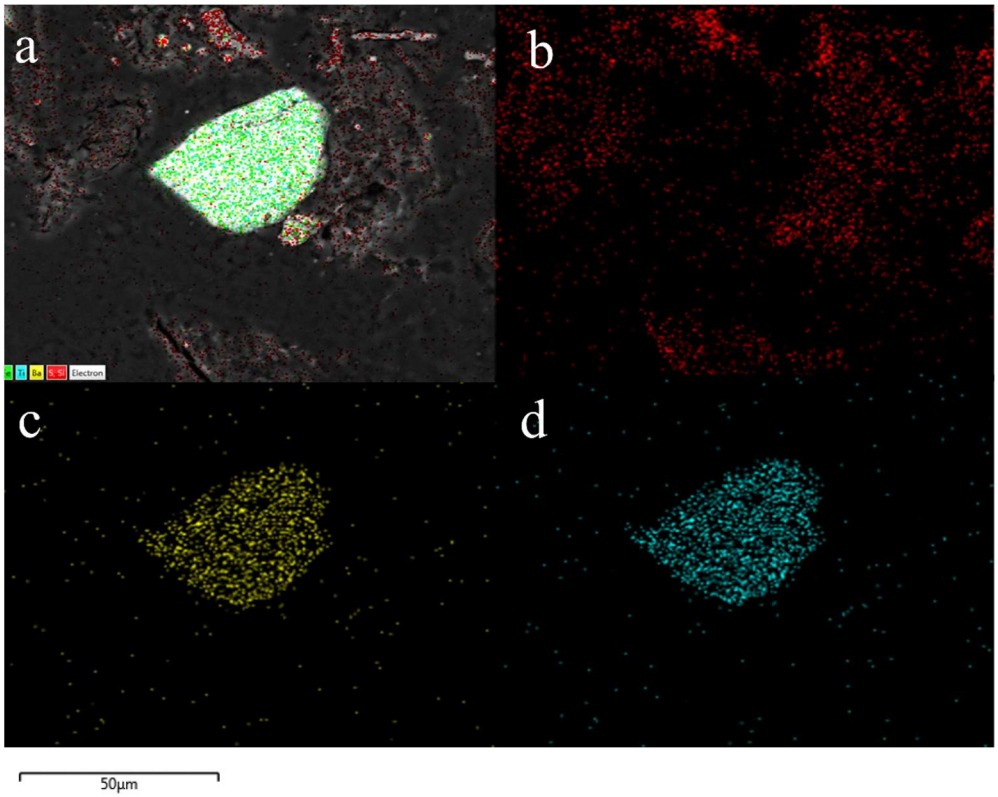

Figure 5.3.5: False colour elemental SEM map of sediment core 4 (0 - 5 cm depth); (a) original image, (b) Si, (c) Ba, (d) Ti.

Chapter 6 Discussion

The aim of this study was to determine whether barium could be applied as a paleo-productivity proxy in a diverse range of environments (freshwater lake, peatland and coastal upwelling). The suitability of barium as an indicator of paleo productivity was determined by recording how barium depth profiles related to other primary productivity proxies (TOC and chlorins). Changes in environmental conditions were recorded by elemental and isotopic proxies (Al, C/N and $\delta^{13}C$), and therefore were utilized to exhibit the changes between allochthonous input and autochthonous production in the different aquatic environments. Hence, if barium is a suitable productivity proxy, it should have reflected these changes in productivity in relation to environmental changes.

Statistical analyses was applied to support or deny the null hypothesis. My null hypothesis is that there is no relationship between two variables (i.e. barium and TOC). Therefore if barium holds a significant and positive relationship with productivity, we can reject this null hypothesis.

SEM analysis was applied to provide further evidence for the relationship of barium and productivity. SEM images were utilized to comment on whether barium is precipitated by biological organisms such as phytoplankton, or whether it chemically precipitates and forms minerals such as barite in the different aquatic environments

6.1 Continental environment: Lake Baikal

Productivity and environmental changes throughout the Holocene: The early-Holocene is defined as a transitioning period from the last glacial maximum coupled with relative climatic stability (Maslin, Stickley and Ettwein, 2001). The environmental conditions of this time were a resultant of numerous forcing procedures such as variable solar intensity, volcanic emissions and ocean-atmospheric interactions. The early-Holocene (10.6 kyr ago) is initiated with a peak concentration (18 000 ppm) of Al (Figure 5.1.5) along with low C/N (Figure 5.1.2) and $\delta^{13}C$ (Figure 5.1.4) and a subtle increase of lake productivity (chlorins and TOC; Figure 5.1.1). These are good indicators of an elevated input of fluvial material into the South Basin sediment profile. This surge allochthonous riverine input is likely a response to the melting of glaciers and permafrost in the surrounding catchment. According to Mackay *et al.* (2017), the early-Holocene experienced intensified summer insolation as a result of orbital alignments. Subsequently, this created a more intense seasonal shift in the central Asian monsoon. Therefore the Siberian region hosted wet and warm summer months, and more intense colder winter months (Mackay *et al.*, 2017). There is a general increased signal of C/N and $\delta^{13}C$ along with a gradual decline in Al concentrations over the early-Holocene (10.3 - 8.8 kyr ago). Based on $\delta^{18}O$ and pollen records from the Vydrino area (Mackay *et al.*, 2011), this period is marked by reduction in river flows and vegetation associated with warm conditions. Although cold and arid conditions prevailed, the lake productivity (TOC and chlorins) gradually increased with elevated diatom concentrations recorded by (Mackay *et al.*, 2017) at 10.3 kyr.

The transition from the early to the mid-Holocene (8.8 -7.3 kyr ago) displays a drastic decline in C/N values to a minima (7.3 Kyr ago) and a gradual increase in lake productivity (TOC and chlorins), indicative of enhanced autochthonous lake productivity as a result of greater input of terrestrial soil material. However, there is a distinct decrease in Al concertation, which initiated from the early-Holocene. Mackay *et al.* (2011) reports low $\delta^{18}O$ values (8.6 - 7.0 kyr ago),

indicative of a decrease in the input of the Selenga River, and similarly White and Bush, (2010) explain that this period is marked by decreased alluvial sedimentation.

An interesting anomaly presents itself in the mid-Holocene (6.8 kyr ago), whereby there is a sharp increase in $\delta^{13}C$ (Figure 5.1.4), TOC (Figure 5.1.1), Al (figure 5.1.5) and C/N (Figure 5.1.2). This phenomenon has been defined by Prokopenko *et al.* (2007) as a mid-Holocene maximum. The organic matter within the lacustrine setting is generally created by the local biota; however, lake productivity is also dependant on terrigenous input of nutrients from the surrounding watershed via river run-off. The primary producers in the water column utilize and recycle these nutrients and compounds, thus an elevated primary productivity is a result of increased alluvial input. Prokopenko *et al.* (2007) suggests that this peak of TOC, is subsequently due to an intensified warm and wet summer climate over the South-eastern Siberian region. There is a subtle peak in TOC, Al and $\delta^{13}C$, and decline in C/N and chlorins over the mid to late- Holocene (5.2 - 4.9 kyr ago), indicating wet climatic conditions dominate over this period, which is interpreted by Mackay *et al.* (2017) as a warming and increased humidity resulting in terrestrial input of organic carbon via meltwaters.

The late-Holocene (4.5 - 1.3 kyr ago) displays a general decline in preserved productivity (TOC and chlorins) and terrestrial input (Al, C/N and $\delta^{13}C$), as compared to the early and mid-Holocene. The decreased allochthonous material is indicative of a decline in precipitation and/or an elevated temperature. Prokopenko *et al.* (2007) defines the Siberian late-Holocene climate as arid due to the persistent extension of the drought-tolerant conifer, Scots Pine. This well-established forest may also explain why there is a decrease in the overall accumulation of carbon (Mackay *et al.*, 2017), as this results in a more stable soil profile in the surrounding catchment thus resulting in a weakening of soil erosion and therefore run-off (Chalov *et al.*, 2012). This shows that drastic changes between main allochthonous input or main autochthonous production occurred during the Holocene in Lake

Baikal that should be reflected in the sedimentary barium, if barium serves as proxy for paleoproductivity.

Barium as a productivity proxy in lacustrine settings: Throughout the Holocene record there are no statistically significant, positive relationships between barium (total and excess) and established productivity proxies (TOC and chlorins). The null hypothesis states that there is no relationship between two variables (i.e. barium and TOC), therefore based on the lack of a significant and positive relationship, we cannot reject the null hypotheses. However, the distribution profiles of total and excess barium display a very similar distribution pattern to productivity proxies at certain periods of time. This study has segmented the Holocene record into smaller time periods, denoted by the early, mid and late-Holocene; and statistical analysis was applied within these periods. This was completed in order to show whether there are any relationships present within these periods, where barium follows a similar distribution as productivity proxies. The total barium profile within the early to late Holocene periods, displayed no significant and positive correlations with productivity proxies. Similarly, the excess barium displayed no significant and positive correlations with productivity proxies over the early and late-Holocene, yet there was a potential positive linear relationship in the mid-Holocene. Because of the lower sample resolution of these time periods, the statistical analysis only represents potential relationships that could hold between the barium profile and the productivity proxies. Consequently, we are only commenting on the suitability of barium as a paleoproductivity proxy based on the statistical analysis applied to the entire Holocene record. Throughout the Holocene there is an observed strong relationship between total barium and aluminium content in the sediment core. This indicates that we can reject the null hypothesis and except an alternative hypothesis, that the two variables (barium and Al concentration) are strongly linked and influence one another.

The SEM analysis displayed no conclusive information on whether barium is associated to the lithogenic or biogenic portion of the sediment, as the barium content of the sediment core was low resolution and was not detected. However barium in the lacustrine system most likely has a lithogenic origin and is most likely introduced by allochthonous material through fluvial deposition. Consequently, barium's sedimentation and ultimately preservation in Lake Baikal is not associated or dependant on the presence of biological material and may not serve as a reliable paleo-productivity proxy. There is a low sedimentation rate in Lake Baikal as recorded by Mackay *et al.* (2017). This is important to note as previously mentioned (section 2.4), in order to form, barite requires the interaction of barium and sulphate super-saturated solution for it to precipitate and transport to the sediment, where it will eventually be preserved (Griffith and Paytan, 2012). However, because the Lake Baikal water column is constantly oxidized (Mackay *et al.*, 2017), this environment does not allow for the formation of a super-saturated sulphate solution to form. Potentially, barite is unable to form as a result of degrading organic matter. Hence, it is not associated or dependant on the presence of biological material and may not serve as a reliable paleo-productivity proxy.

6.2 Continental environment: Mfabeni peatland

Productivity and environmental changes throughout the Holocene and modern environment: The shift from the last glacial maximum into the interglacial Holocene period, is met with great climatic variability (Baker *et al.*, 2014). There are many pronounced fluctuations of productivity (TOC) and fluvial input (Al) in the Mfabeni peatland over the Holocene. Over the early-Holocene, there is a general increase in the concentrations of Al (12 - 9.8 kyr ago) and TOC (10.4 - 8.7 kyr ago). Baker *et al.* (2014) similarly reports increased accumulation rates of carbon during this same period. Therefore there is an elevated rate of sedimentation via precipitation and river run-off, as these are the main inputs in the peatland (Chaudhary, Miller and Smith, 2017). There is sudden drop in the Al content at 9.1 kyr ago. Holmgren *et al.*, (2003) records a distinctive decline and minimum values of $\delta^{13}C$ over this period. Variation of $\delta^{13}C$ values have been interpreted as a reflection of the atmospheric changes such as moisture, precipitation and temperature. Therefore low values of $\delta^{13}C$ indicate a reduction of C_4 plant species (i.e. grassland) and a growth of C_3 plant species (i.e. trees and small shrubs). From this we can deduce that this period displays a low organic content and poor-vegetation cover as a result of a dry/arid environment (Holmgren *et al.*, 2003).

The Mid-Holocene is marked with two distinctive anticlines for both the TOC and Al content, at 7.1 kyr and 5.1 kyr ago. These are signals of low accumulation of carbon, low level of productivity and decreased precipitation. Similarly, Norström *et al.*, (2009) recorded low accumulation rates over (7.5 - 2.5 kyr ago), relating this to an increased drought environment as a result of elevated temperatures. A thermal maximum is also reported by Chevalier and Chase (2015) over the mid-Holocene (7 kyr ago). However, after this temperature peak, Chevalier and Chase, (2015) record a gradual decline in temperature. This cool and dry event is continuous until 5.1 kyr, and is exhibited by the $\delta^{13}C$ values of Finch and Hill (2008). Through the decrease of Podocarpus forest pollen and increase of Poaceae pollen, Finch and

Hill (2008) deduce a dominant grassland/savannah plant species therefore indicating a cool and dry environment.

The early-Holocene (5 - 2.2 kyr ago) exhibits a gradual increase and maximum peaks of TOC (51 000 ppm) and Al (44 000 ppm) concentrations. After 5 kyr, Chevalier and Chase, (2015) records a rapid increase of precipitation. This is confirmed by Baker *et al.* (2014), with an enriched $\delta^{13}C$ signal and increased carbon accumulation, indicative of a spike of C_4 plant species. Therefore we can deduce that this area endured intense water-logging due to warm and moist environmental conditions. This was followed by a cooling event (2.2 - 1.5 kyr ago), similar to 5.4 kyr and 7.1 kyr events, whereby, there is a sudden drop in productivity and sedimentation due to increased aridity (Baker *et al.*, 2014).

Barium as a productivity proxy in wetland settings: There is no positive and significant relationship observed between barium (total and excess) and productivity (TOC) throughout the Holocene record. The distribution profiles display opposite trend lines throughout the record. There is no positive, linear relationship between barium and the productivity proxy over the early-Holocene, mid-Holocene, late-Holocene or the modern environment. The null hypothesis states that there is no relationship between two variables (i.e. barium and TOC), therefore, because there is no significant and positive relationship between barium and the productivity proxy (TOC), we cannot reject the null hypotheses. Hence, barium cannot serve as a suitable productivity proxy.

Conversely, there is a positive relationship between total barium and Al content throughout the Holocene, and is statistically significant. Therefore we can reject the null hypothesis and accept the alternative hypothesis. The alternative hypothesis states that barium and Al exhibit a positive linear trend and therefore there is a relationship between them. Thus barium is strongly associated with the aluminosilicate fraction, as the Al content was utilized to infer the

lithogenic material within the environment. Based on this study, barium shows no potential as a suitable paleoproductivity proxy in peatland environments. Baker *et al.* (2014) reports that the formation of the peat deposits is highly dependent on water-logging conditions. Consequently, peatlands are host to an anoxic environment (Sieben, 2019). As previously mentioned (section 2.4) reducing environmental conditions, resulting in the redistribution of barium contents into the sediment pore water and the sediment-water interface. This resuspension of barium contents back into the water column, allows once more for the deposition of barium. However, this may cause difficulty with interpretation of results, as barium contents redeposit under different environmental conditions and productivity (Tribovillard *et al.*, 1996), rendering it not a suitable proxy for paleoproductivity.

6.3 Coastal marine environment: off-shore Namibia

Productivity and environmental changes throughout the modern environment: The productivity in the sediment cores is represented by the concentration of chlorins, which fluctuates throughout all four sediment cores. In the North Namibian cell (core 1; 20°02 S) and Central Namibian cell (core 3; 23°02 S), there is an increase in chlorins concertation over the surface sediment (0 – 5 cm) depth and a decrease over the (5 – 10 cm) depth. Similarly, the North Namibian cell (core 3; 23°02 S) and Central Namibian cell (core 4; 23°20 S) exhibit a decline in chlorins over the (5 – 10 cm depth). Over the sediment (10 – 15 cm) depth, both the North Namibian cell (core 1; 20°02 S) and Central Namibian cell (core 4; 23°20 S) exhibit an increase in productivity. Fluctuations in productivity in surface sediment cores have been recorded by (Struck *et al.*, 2002), and display similar distributions of productivity throughout the sediment profile to this study. Struck *et al.*, (2002) utilizes TOC, carbon isotope ($\delta^{13}C$) and nitrogen isotope ($\delta^{15}N$) to infer productivity. $\delta^{13}C$ is used as an

indicator for variation in the dissolved carbon dioxide within upwelling waters (Struck *et al.*, 2002), therefore lower dissolved carbon dioxide is indicative of higher productivity (Struck *et al.*, 2002).

The lithogenic input into the upwelling cells is represented by the Al concentration, which displays variability throughout the sediments cores. There is a general decrease of lithogenic input towards the surface sediment depths in the North Namibian upwelling cell and an increase in the Central Namibian upwelling cell. Emeis *et al.*, (2009) records a significant sedimentation variation over the past 100 years, as sea surface temperature have increased by 1° C in the Northern cell, and decreased by 1°C in the Central Namibian cell. Therefore upwelling activity has increased in the Central cell and decreased in the Northern Namibian cell. Variability in the upwelling cell activity and ultimately sedimentation is greatly dependant on the southeast trade winds, as wind stress is the main driver of the upwelling system (Silió-Calzada *et al.*, 2008). Therefore, this could potentially explain why the Central Namibian upwelling cell is dominated by lithogenic input in comparison to the North Namibian upwelling cell.

Barium as a productivity proxy in coastal setting: The sample resolution for the coastal upwelling environment was very low, therefore the statistical relationships discussed are only meant represent potential relationships between barium, productivity proxy and aluminium. Barium displayed no positive linear relationship in the Central Namibian upwelling cell throughout the modern environment profile. Whereas, the barium and Al relationship was very strong, statistically significant and positive throughout the sediment profile, potentially indicating a lithogenic source of barium. Therefore we cannot reject the null hypothesis, therefore barium does not serve as a suitable paleoproductivity proxy in the Central Namibian upwelling cell environment. However, in the North Namibian upwelling the excess barium

exhibited a significantly strong and positive correlation with chlorins throughout the sediment core. Therefore we can reject the null hypotheses, and thus barium serve as a suitable productivity proxy. However, what is interesting to observe, was the strong positive correlation between total barium and Al content throughout core 2 (20°30 S). Because the total barium concentration is composed of a biogenic and lithogenic portion, and the biogenic portion (excess barium) displays a positive linear relationship with productivity (chlorins) we can reject the null hypothesis. Hence, barium is a suitable paleoproductivity in core 2 (20°30 S) of the North Namibian cell (NNC; 20° S).The SEM analysis confirmed that barium is only associated with the alluminosillicate fraction for Central Namibian cell. Whereas, barium is associated with the alluminosillicate and biological fraction of the North Namibian cell, this broad distribution of the barium results in an inconclusive interpretation of the North Namibian cell SEM images.

Chapter 7 conclusion

The aim of this study was to determine whether barium is a suitable and reliable tool to apply when reconstructing paleoproductivity in various environments over the Holocene and modern environment. The application of barium as an alternative measure for recording past productivity has been executed in many marine environments. However, it has rarely be explored in freshwater systems, thus the main objective of this study was to provide new data for a suite of environments. Through the review of previously published literature, the formation, transportation and preservation of organic matter was established in lacustrine and marine environments. The application of barium as a productivity proxy was reviewed in modern and past ocean settings, therefore the advantages and disadvantages of barium as a paleo-productivity proxy have been established. Barium records were constructed for lacustrine, peatland and coastal marine environments through ICP-MS and XRF analysis. These datasets were compared to established paleoproductivity proxy data from previously published literature. Simple statistical analysis was applied to the datasets in order to define a positive linear relationship between barium and productivity, therefore to establish whether barium follows a similar distribution pattern as other productivity proxies. Scanning Electron Microscope (SEM) analysis was employed to determine the elemental distribution throughout the sediment record. The aim of this was to determine whether barium is precipitated by biological organisms or whether it chemically precipitates and forms minerals. Depth profiles were constructed for total barium and excess barium, where excess barium represented the biogenic fraction of the total barium concentration. These profiles were compared to various other productivity, elemental and isotopic proxy profiles for lacustrine (Lake Baikal), peatland (Mfabeni peat) and coastal (Benguela upwelling cell) settings. The profiles for the continental settings (lacustrine and peatland) exhibited no evidence for a positive linear relationship between barium and productivity proxies. Therefore barium was not a suitable

proxy to apply in reconstructing the paleoproductivity in these settings. Similarly, the barium profiles of the Central Namibian coastal marine setting displayed no positive linear relationship with productivity. However, the barium profiles in the North Namibian Cell displayed a potential positive and significant linear relationship with other productivity proxies, therefore displaying the potential for the use of barium as a suitable proxy for productivity. This research aimed to identify barium as a suitable productivity proxy in a wide range of environments. Though it was not successful at defining a linear relationship for barium and productivity proxies, this study did effectively establish potential relationships between barium and paleoproductivity in certain periods of the Holocene record.

7.1 Recommendations

The main limitation of this study was the small sample size, which resulted in a low resolution of results. Thus there was a lack of accuracy in the statistical analysis, as this study was only able to comment on the suitability of barium based on the whole Holocene record in comparison to the potential relationships present in the specific time periods. Therefore future research should focus on testing whether these potential relationships hold between barium and paleoproductivity proxies and whether they are accurate with higher resolution studies. This research study proved that barium was an unreliable proxy to reconstruct paleoproductivity for various environments, however it did not take into account the reconstruction of various environmental factors which could potentially influence the behaviour of barium. For future research we suggest that a multiproxy approach be considered for such a study, as it is important to understand what the variations of environmental conditions, such as the redox environment, are throughout the Holocene record. This could potentially explain some of the relationships present between barium and paleoproductivity proxies.

References

Babu, C. P. *et al.* (2002) 'Barium as a productivity proxy in continental margin sediments: A study from the eastern Arabian Sea', *Marine Geology*, 184(3–4), pp. 189–206. doi: 10.1016/S0025-3227(01)00286-9.
Baker, A. *et al.* (2014) 'Geochemical records of palaeoenvironmental controls on peat forming processes in the Mfabeni peatland, Kwazulu Natal, South Africa since the Late Pleistocene', *Palaeogeography, Palaeoclimatology, Palaeoecology*, 395, pp. 95–106. doi: 10.1016/j.palaeo.2013.12.019.
Baker, A. *et al.* (2017) 'Climatic variability in Mfabeni peatlands (South Africa) since the late Pleistocene', *Quaternary Science Reviews*. Elsevier Ltd, 160, pp. 57–66. doi: 10.1016/j.quascirev.2017.02.009.
Baker, A., Routh, J. and Roychoudhury, A. N. (2016) 'Biomarker records of palaeoenvironmental variations in subtropical Southern Africa since the late Pleistocene: Evidences from a coastal peatland', *Palaeogeography, Palaeoclimatology, Palaeoecology*. Elsevier B.V., 451, pp. 1–12. doi: 10.1016/j.palaeo.2016.03.011.
Barange, M., Pillar, S. C. and Hutchings, L. (1992) 'Major pelagic borders of the Benguela upwelling system according to euphausiid species distribution', *South African Journal of Marine Science*, 12(1), pp. 3–17. doi: 10.2989/02577619209504686.
Bonny, S. M. and Jones, B. (2007) 'Diatom-mediated barite precipitation in microbial mats calcifying at Stinking Springs, a warm sulphur spring system in Northwestern Utah, USA', *Sedimentary Geology*, 194(3–4), pp. 223–244. doi: 10.1016/j.sedgeo.2006.06.007.
Brook, A. J. *et al.* (1980) 'Barium accumulation by desmids of the genus closterium (Zygnemaphyceae)', *British Phycological Journal*, 15(3), pp. 261–264. doi: 10.1080/00071618000650251.
Burdige, D. J. (2007) 'Preservation of organic matter in marine sediments: Controls, mechanisms, and an imbalance in sediment organic carbon budgets?', *Chemical Reviews*, 107(2), pp. 467–485. doi: 10.1021/cr050347q.
Canfield, D. E. (1994) 'Factors influencing organic carbon preservation in marine sediments', *Chemical Geology*, 114(3–4), pp. 315–329. doi: 10.1016/0009-2541(94)90061-2.
Canfield, D. E. and Thamdrup, B. (2009) 'Towards a consistent classification scheme for geochemical environments, or, why we wish the term "suboxic" would go away: Editorial', *Geobiology*, 7(4), pp. 385–392. doi: 10.1111/j.1472-4669.2009.00214.x.
Chalov, S. *et al.* (2012) 'Suspended and Dissolved Matter Fluxes in the Upper Selenga River Basin', *Geography, Environment, Sustainability*, 5(2), pp. 78–94. doi: 10.24057/2071-9388-2012-5-2-78-94.
Charlet, F. *et al.* (2005) 'Sedimentary dynamics on isolated highs in Lake Baikal: Evidence from detailed high-resolution geophysical data and sediment cores', *Global and Planetary Change*, 46(1-4 SPEC. ISS.), pp. 125–144. doi: 10.1016/j.gloplacha.2004.11.009.
Chaudhary, N., Miller, P. A. and Smith, B. (2016) 'Modelling Holocene peatland dynamics with an individual-based dynamic vegetation model', *Biogeosciences Discussions*, (December), pp. 1–46. doi: 10.5194/bg-2016-319.
Chaudhary, N., Miller, P. A. and Smith, B. (2017) 'Modelling Holocene peatland dynamics with an individual-based dynamic vegetation model', *Biogeosciences*, 14(10), pp. 2571–2596. doi: 10.5194/bg-14-2571-2017.
Chevalier, M. and Chase, B. M. (2015) 'Southeast African records reveal a coherent shift from high- to low-latitude forcing mechanisms along the east African margin across last glacial-interglacial transition', *Quaternary Science Reviews*. Elsevier Ltd, 125, pp. 117–130. doi: 10.1016/j.quascirev.2015.07.009.

Chow, Tsaihwa; Goldberg, E. D. (1976) 'On the marine geochemistry of barium', *Marine Chemistry*, 4(2), pp. 141–154. doi: 10.1016/0304-4203(76)90003-7.
Clulow, A. D. *et al.* (2013) 'Water-use dynamics of a peat swamp forest and a dune forest in Maputaland, South Africa', *Hydrology and Earth System Sciences*, 17(5), pp. 2053–2067. doi: 10.5194/hess-17-2053-2013.
Clymo, R. S., Turunen, J. and Tolonen, K. (1998) 'Carbon Accumulation in Peatland', *Oikos*, 81(2), p. 368. doi: 10.2307/3547057.
Coffey, M. *et al.* (1997) 'The Behaviour of Dissolved Barium in Estuaries', *Estuarine, Coastal and Shelf Science*, 45(1), pp. 113–121. doi: 10.1006/ecss.1996.0157.
Colman, S. M., Karabanov, E. B. and Nelson, C. H. (2003) 'Quaternary sedimentation and subsidence history of Lake Baikal, Siberia, based on seismic stratigraphy and coring', *Journal of Sedimentary Research*, 73(6), pp. 941–956. doi: 10.1306/041703730941.
Contreras, S. *et al.* (2018) 'Organic matter geochemical signatures (TOC, TN, C/N ratio, δ13C and δ15N) of surface sediment from lakes distributed along a climatological gradient on the western side of the southern Andes', *Science of the Total Environment*. Elsevier B.V., 630, pp. 878–888. doi: 10.1016/j.scitotenv.2018.02.225.
Dean, W. E. and Gorham, E. (1998) 'Magnitude and significance of carbon burial in lakes, reservoirs, and peatlands', *Geology*, 26(6), pp. 535–538. doi: 10.1130/0091-7613(1998)026<0535:MASOCB>2.3.CO;2.
Demory, F. *et al.* (2005) 'Detrital input and early diagenesis in sediments from Lake Baikal revealed by rock magnetism', *Global and Planetary Change*, 46(1-4 SPEC. ISS.), pp. 145–166. doi: 10.1016/j.gloplacha.2004.11.010.
Dymond, J., Suess, E. and Lyle, M. (1992a) 'Barium in the deep-sea sediment: A geochemical proxy for paleoproductivity', *Paleoceanography*, 7(3), pp. 391–391. doi: 10.1029/92PA01080.
Dymond, J., Suess, E. and Lyle, M. (1992b) 'Correction to "Barium in the deep-sea sediment: A geochemical proxy for paleoproductivity"', *Paleoceanography*, 7(3), pp. 391–391. doi: 10.1029/92PA01080.
Emeis, K. *et al.* (2018) 'Biogeochemical processes and turnover rates in the Northern Benguela Upwelling System', *Journal of Marine Systems*, 188(December 2016), pp. 63–80. doi: 10.1016/j.jmarsys.2017.10.001.
Emeis, K. C. *et al.* (2009) 'Variability in upwelling intensity and nutrient regime in the coastal upwelling system offshore Namibia: Results from sediment archives', *International Journal of Earth Sciences*, 98(2), pp. 309–326. doi: 10.1007/s00531-007-0236-5.
Fagel, N. and Boës, X. (2008) 'Clay-mineral record in Lake Baikal sediments: The Holocene and Late Glacial transition', *Palaeogeography, Palaeoclimatology, Palaeoecology*, 259(2–3), pp. 230–243. doi: 10.1016/j.palaeo.2007.10.009.
Falkner, K. K. *et al.* (1997) 'Minor and trace element chemistry of Lake Baikal, its tributaries, and surrounding hot springs', *Limnology and Oceanography*, 42(2), pp. 329–345. doi: 10.4319/lo.1997.42.2.0329.
Falkowski, P. G. *et al.* (2003) 'Phytoplankton and Their Role in Primary, New, and Export Production', *Ocean Biogeochemistry*, pp. 99–121. doi: 10.1007/978-3-642-55844-3_5.
Fenner, N., Freeman, C. and Reynolds, B. (2005) 'Observations of a seasonally shifting thermal optimum in peatland carbon-cycling processes; implications for the global carbon cycle and soil enzyme methodologies', *Soil Biology and Biochemistry*, 37(10), pp. 1814–1821. doi: 10.1016/j.soilbio.2005.02.032.
Fiedler, S., Vepraskas, M. J. and Richardson, J. L. (2007) 'Soil Redox Potential: Importance, Field Measurements, and Observations', *Advances in Agronomy*, 94(06), pp. 1–54. doi: 10.1016/S0065-2113(06)94001-2.
Finch, J. M. (2005) *Late Quaternary palaeoenvironments of the Mfabeni Peatland, northern*

KwaZulu-Natal, *School of Environmental Sciences*. University of KwaZulu-Natal. Available at: http://hdl.handle.net/10413/1944.
Finch, J. M. and Hill, T. R. (2008) 'A late Quaternary pollen sequence from Mfabeni Peatland, South Africa: Reconstructing forest history in Maputaland', *Quaternary Research*. University of Washington, 70(3), pp. 442–450. doi: 10.1016/j.yqres.2008.07.003.
Finlay, B. J., Hetherington, N. B. and Da Vison, W. (1983) 'Active biological participation in lacustrine barium chemistry', *Geochimica et Cosmochimica Acta*, 47(7), pp. 1325–1329. doi: 10.1016/0016-7037(83)90071-6.
Francois, R., Manganini, J. and Ravizza, E. (1995) 'Pnew =', 9(2), pp. 289–303.
Fritz, L. *et al.* (1990) 'Biomineralization of barite in the shell of teh freshwater asiatic clam Corbicula fluminea (Mollusca : Bivalvia)', *Limnology and oceanography*, 35(3), pp. 756–762. doi: 10.2307/2837626.
Ganeshram, R. S. (2006) 'Factors Controlling the Burial of Organic Carbon in Laminated and Bioturbated Sediments off NW Mexico', *Mineralogical Magazine*. Mineralogical Society, 62A(1), pp. 495–495. doi: 10.1180/minmag.1998.62a.1.262.
Gonza, M. T., Chekroun, K. Ben and Paytan, A. (2003) 'Precipitation of Barite by', *American Society for Microbiology*, 69(9), pp. 5722–5725. doi: 10.1128/AEM.69.9.5722.
Gorham, E. (1991) 'Northern peatlands: role in the carbon cycle and probable responses to climatic warming', *Ecological Applications*, 1(2), pp. 182–195. doi: 10.2307/1941811.
Griffith, E. M. and Paytan, A. (2012) 'Barite in the ocean - occurrence, geochemistry and palaeoceanographic applications', *Sedimentology*, 59(6), pp. 1817–1835. doi: 10.1111/j.1365-3091.2012.01327.x.
Grundling, P. *et al.* (2013) 'Development and persistence of an African mire: How the oldest South African fen has survived in a marginal climate', *Catena*. Elsevier B.V., 110, pp. 176–183. doi: 10.1016/j.catena.2013.06.004.
Grundling, P. L. *et al.* (2015) 'Quantifying the water balance of Mfabeni mire (Isimangaliso wetland park, South Africa) to understand its importance, functioning and vulnerability', *Mires and Peat*, 16, pp. 1–18.
Gudasz, C. *et al.* (2010) 'Temperature-controlled organic carbon mineralization in lake sediments', *Nature*. Nature Publishing Group, 466(7305), pp. 478–481. doi: 10.1038/nature09186.
Hanor, J. S. and Chan, L. H. (1977) 'Non-conservative behavior of barium during mixing of Mississippi River and Gulf of Mexico waters', *Earth and Planetary Science Letters*, 37(2), pp. 242–250. doi: 10.1016/0012-821X(77)90169-8.
Hedges, J. I., Keil, R. G. and Benner, R. (1997) 'What happens to terrestrial organic matter in the ocean?', *Organic Geochemistry*, 27(5–6), pp. 195–212. doi: 10.1016/S0146-6380(97)00066-1.
Heim, B. *et al.* (2005) 'Variation in Lake Baikal's phytoplankton distribution and fluvial input assessed by SeaWiFS satellite data', *Global and Planetary Change*, 46(1-4 SPEC. ISS.), pp. 9–27. doi: 10.1016/j.gloplacha.2004.11.011.
Henderson, G. M. (2002) 'New oceanic proxies for paleoclimate', *Earth and Planetary Science Letters*, 203(1), pp. 1–13. doi: 10.1016/S0012-821X(02)00809-9.
Hollerbach, A. and Dehmer, J. (1994) 'Diagenesis of organic matter', *Developments in Sedimentology*, 51(C), pp. 309–359. doi: 10.1016/S0070-4571(08)70443-6.
Holmgren, K. *et al.* (2003) 'Persistent millennial-scale climatic variability over the past 25,000 years in Southern Africa', *Quaternary Science Reviews*, 22(21–22), pp. 2311–2326. doi: 10.1016/S0277-3791(03)00204-X.
Holzwarth, U., Esper, O. and Zonneveld, K. (2007) 'Distribution of organic-walled dinoflagellate cysts in shelf surface sediments of the Benguela upwelling system in relationship to environmental conditions', *Marine Micropaleontology*, 64(1–2), pp. 91–119.

doi: 10.1016/j.marmicro.2007.04.001.
Horner, T. J. *et al.* (2017) 'Pelagic barite precipitation at micromolar ambient sulfate', *Nature Communications*. Springer US, 8(1), pp. 1–11. doi: 10.1038/s41467-017-01229-5.
Hutchings, L. *et al.* (2009) 'The Benguela Current: An ecosystem of four components', *Progress in Oceanography*. Elsevier Ltd, 83(1–4), pp. 15–32. doi: 10.1016/j.pocean.2009.07.046.
Jeandel, C. *et al.* (2000) 'Biogenic barium in suspended and trapped material as a tracer of export production in the tropical NE Atlantic (EUMELI sites)', *Marine Chemistry*, 71(1–2), pp. 125–142. doi: 10.1016/S0304-4203(00)00045-1.
Kandasamy, S. and Nath, B. N. (2016) 'Perspectives on the terrestrial organic matter transport and burial along the land-deep sea continuum: Caveats in our understanding of biogeochemical processes and future needs', *Frontiers in Marine Science*, 3(DEC), pp. 1–18. doi: 10.3389/fmars.2016.00259.
Kukulus, M. (2004) *A quantitative approach to the evolution of the central Walvis Basin offshore NW-Namibia: structure, mass balancing, and hydrocarbon potential*. Universität Würzburg. Available at: http://eprints.uanl.mx/5481/1/1020149995.PDF.
Lazarus, D. *et al.* (2006) 'Comparison of radiolarian and sedimentologic paleoproductivity proxies in the latest Miocene-Recent Benguela Upwelling System', *Marine Micropaleontology*, 60(4), pp. 269–294. doi: 10.1016/j.marmicro.2006.06.003.
Liguori, B. T. P., De Almeida, M. G. and de Rezende, C. E. (2016) 'Barium and its importance as an indicator of (Paleo)productivity', *Anais da Academia Brasileira de Ciencias*, 88(4), pp. 2093–2103. doi: 10.1590/0001-3765201620140592.
Limpens, J. *et al.* (2008) 'Peatlands and the carbon cycle: From local processes to global implications - A synthesis', *Biogeosciences*, 5(5), pp. 1475–1491. doi: 10.5194/bg-5-1475-2008.
Mackay, A. W. *et al.* (2011) 'A reassessment of late glacial - Holocene diatom oxygen isotope record from Lake Baikal using a geochemical mass-balance approach', *Journal of Quaternary Science*, 26(6), pp. 627–634. doi: 10.1002/jqs.1484.
Mackay, A. W. *et al.* (2017) 'Holocene carbon dynamics at the forest–steppe ecotone of southern Siberia', *Global Change Biology*, 23(5), pp. 1942–1960. doi: 10.1111/gcb.13583.
Martinez-Ruiz, F. *et al.* (2015) 'Paleoclimate and paleoceanography over the past 20,000yr in the Mediterranean Sea Basins as indicated by sediment elemental proxies', *Quaternary Science Reviews*, 107, pp. 25–46. doi: 10.1016/j.quascirev.2014.09.018.
Maslin, M., Stickley, C. and Ettwein, V. (2001) 'Holocene Climate Variability', *Encyclopedia of Ocean Sciences: Second Edition*, pp. 125–132. doi: 10.1016/B978-012374473-9.00246-0.
McManus, J. *et al.* (1994) 'Remobilization of barium in continental margin sediments', *Geochimica et Cosmochimica Acta*, 58(22), pp. 4899–4907. doi: 10.1016/0016-7037(94)90220-8.
Meyers, P. A. (no date) *Organic geochemical proxies of paleoceanographic, paleolimnologic, and paleoclimatic processes*.
Meyers, P. A. and Ishiwatari, R. (1993) 'The early diagenesis of organic matter in lacustrine sediments', *Organic geochemistry: principles and applications*, pp. 185–209. doi: 10.1007/978-1-4615-2890-6_8.
Meysman, F. J. R., Middelburg, J. J. and Heip, C. H. R. (2006) 'Bioturbation: a fresh look at Darwin's last idea', *Trends in Ecology and Evolution*, 21(12), pp. 688–695. doi: 10.1016/j.tree.2006.08.002.
Miller, C. *et al.* (2019) 'Late quaternary climate variability at mfabeni peatland, eastern south africa', *Climate of the Past*, 15(3), pp. 1153–1170. doi: 10.5194/cp-15-1153-2019.
Millero, F. J. *et al.* (2008) 'The composition of Standard Seawater and the definition of the

Reference-Composition Salinity Scale', *Deep-Sea Research Part I: Oceanographic Research Papers*, 55(1), pp. 50–72. doi: 10.1016/j.dsr.2007.10.001.
Mollenhauer, G. *et al.* (2002) 'Glacial/interglacial variablity in the Benguela upwelling system: Spatial distribution and budgets of organic carbon accumulation', *Global Biogeochemical Cycles*, 16(4), pp. 81-1-81–15. doi: 10.1029/2001gb001488.
Monnin, C. *et al.* (1999) 'The marine barite saturation state of the world's oceans', *Marine Chemistry*, 65(3–4), pp. 253–261. doi: 10.1016/S0304-4203(99)00016-X.
Nardini, P. *et al.* (2019) *The tropical-subtropical coupling in the Southeast Atlantic from the perspective of the northern Benguela upwelling system*, *PLoS ONE*. doi: 10.1371/journal.pone.0210083.
Niedermeier, M., Gierlinger, N. and Lütz-Meindl, U. (2018) 'Biomineralization of strontium and barium contributes to detoxification in the freshwater alga Micrasterias', *Journal of Plant Physiology*. Elsevier GmbH., 230, pp. 80–91. doi: 10.1016/j.jplph.2018.08.008.
Norström, E. *et al.* (2009) 'Reconstruction of environmental and climate changes at Braamhoek wetland, eastern escarpment South Africa, during the last 16,000 years with emphasis on the Pleistocene-Holocene transition', *Palaeogeography, Palaeoclimatology, Palaeoecology*. Elsevier B.V., 271(3–4), pp. 240–258. doi: 10.1016/j.palaeo.2008.10.018.
Och, L. M. *et al.* (2014) 'Rare earth elements in the sediments of Lake Baikal', *Chemical Geology*. Elsevier B.V., 376, pp. 61–75. doi: 10.1016/j.chemgeo.2014.03.018.
Och, L. M. *et al.* (2016) 'Elevated uranium concentrations in Lake Baikal sediments: Burial and early diagenesis', *Chemical Geology*. Elsevier B.V., 441, pp. 92–105. doi: 10.1016/j.chemgeo.2016.08.001.
Paytan, A. *et al.* (2003) 'Selective phosphorus regeneration of sinking marine particles: Evidence from 31P-NMR', *Marine Chemistry*. Elsevier, 82(1–2), pp. 55–70. doi: 10.1016/S0304-4203(03)00052-5.
Paytan, A. and Griffith, E. M. (2007) 'Marine barite: Recorder of variations in ocean export productivity', *Deep-Sea Research Part II: Topical Studies in Oceanography*, 54(5–7), pp. 687–705. doi: 10.1016/j.dsr2.2007.01.007.
Pfeifer, K., Kasten, S., Hensen, C. and Schulz, Horst D. (2001) 'Reconstruction of primary productivity from the barium contents in surface sediments of the South Atlantic Ocean', in *Marine Geology*, pp. 13–24. doi: 10.1016/S0025-3227(01)00121-9.
Pfeifer, K., Kasten, S., Hensen, C. and Schulz, Horst D (2001) 'Reconstruction of primary productivity from the barium contents in surface sediments of the South Atlantic Ocean', 177.
Pitcher, G. C., Brown, P. C. and Mitchell-Innes, B. A. (1992) 'Spatio-temporal variability of phytoplankton in the southern Benguela upwelling system', *South African Journal of Marine Science*, 12(1), pp. 439–456. doi: 10.2989/02577619209504717.
Prokopenko, A. A. *et al.* (2007) 'Paleoenvironmental proxy records from Lake Hovsgol, Mongolia, and a synthesis of Holocene climate change in the Lake Baikal watershed', *Quaternary Research*, 68(1), pp. 2–17. doi: 10.1016/j.yqres.2007.03.008.
Rieder, N. *et al.* (1982) 'X-ray Microanalysis of the Mineral Contents of Some Protozoa', *The Journal of Protozoology*, 29(1), pp. 15–18. doi: 10.1111/j.1550-7408.1982.tb02875.x.
Sageman, B. (2009) 'Ocean anoxic events', *Encyclopedia of Earth Sciences Series*, pp. 185–198. doi: 10.1007/978-1-4020-4411-3_155.
Schoepfer, S. D. *et al.* (2015) 'Total organic carbon, organic phosphorus, and biogenic barium fluxes as proxies for paleomarine productivity', *Earth-Science Reviews*. Elsevier, pp. 23–52. doi: 10.1016/j.earscirev.2014.08.017.
Senko, J. M. *et al.* (2004) 'Barite deposition resulting from phototrophic sulfide-oxidizing bacterial activity', *Geochimica et Cosmochimica Acta*, 68(4), pp. 773–780. doi: 10.1016/j.gca.2003.07.008.

Shigemitsu, M. *et al.* (2007) 'Ba, Si, U, Al, Sc, La, Th, C and 13C/12C in a sediment core in the western subarctic Pacific as proxies of past biological production', *Marine Chemistry*, 106(3–4), pp. 442–455. doi: 10.1016/j.marchem.2007.04.004.
Sieben, E. J. J. (2019) 'Zonal and azonal vegetation revisited: How is wetland vegetation distributed across different zonobiomes', *Austral Ecology*, 44(3), pp. 449–460. doi: 10.1111/aec.12679.
Siegel, H. *et al.* (2007) 'Identification of coccolithophore blooms in the SE Atlantic Ocean off Namibia by satellites and in-situ methods', *Continental Shelf Research*, 27(2), pp. 258–274. doi: 10.1016/j.csr.2006.10.003.
Siegel, H., Ohde, T. and Gerth, M. (2014) 'Remote Sensing of the African Seas', *Remote Sensing of the African Seas*, pp. 167–183. doi: 10.1007/978-94-017-8008-7.
Silió-Calzada, A. *et al.* (2008) 'Estimation of new primary production in the Benguela upwelling area, using ENVISAT satellite data and a model dependent on the phytoplankton community size structure', *Journal of Geophysical Research: Oceans*, 113(11), pp. 1–19. doi: 10.1029/2007JC004588.
Sobek, S. et al (2009) 'Organic carbon burial efficiency in lake sediments controlled by oxygen exposure time and sediment source', *Limnology and Oceanography,* 54(6), pp. 2243–2254. doi: 10.1109/TAES.2015.140638.
Stavreva, R. (1986) 'Final version', *Microelectronics Journal*, 17(2), p. 45. Available at: https://linkinghub.elsevier.com/retrieve/pii/S0026269286800167.
Stecher, H. A. and Kogut, M. B. (1999) 'Rapid barium removal in the Delaware estuary', *Geochimica et Cosmochimica Acta*, 63(7–8), pp. 1003–1012. doi: 10.1016/S0016-7037(98)00310-X.
Struck, U. *et al.* (2002) 'Changes of the upwelling rates of nitrate preserved in the δ15N-signature of sediments and fish scales from the diatomaceous mud belt of Namibia', *Geobios*, 35(1), pp. 3–11. doi: 10.1016/S0016-6995(02)00004-9.
Taylor, R. *et al.* (2006) 'Groundwater-dependent ecology of the shoreline of the subtropical Lake St Lucia estuary', *Environmental Geology*, 49(4), pp. 586–600. doi: 10.1007/s00254-005-0095-y.
Tribovillard, N. *et al.* (2006) 'Trace metals as paleoredox and paleoproductivity proxies: An update', *Chemical Geology*, 232(1–2), pp. 12–32. doi: 10.1016/j.chemgeo.2006.02.012.
Tribovillard, N. P. *et al.* (1996) 'Lack of organic matter accumulation on the upwelling-influenced Somalia margin in a glacial-interglacial transition', *Marine Geology*, 133(3–4), pp. 157–182. doi: 10.1016/0025-3227(96)00034-5.
Tyson, R. V. (2011) 'The "Productivity Versus Preservation" Controversy: Cause, Flaws, and Resolution', *Deposition of Organic-Carbon-Rich Sediments: Models*, (82), pp. 17–33. doi: 10.2110/pec.05.82.0017.
Wang, S. *et al.* (2019) 'Redox-driven shifts in soil microbial community structure in the drawdown zone after construction of the Three Gorges Dam', *Soil Ecology Letters*, 1(3–4), pp. 114–125. doi: 10.1007/s42832-019-0005-y.
Wania, R., Ross, I. and Prentice, I. C. (2009) 'Integrating peatlands and permafrost into a dynamic global vegetation model: 2. Evaluation and sensitivity of vegetation and carbon cycle processes', *Global Biogeochemical Cycles*, 23(3), p. n/a-n/a. doi: 10.1029/2008gb003413.
Wilcock, J. R. *et al.* (1989) 'Biological minerals formed from strontium and barium sulphates. II. Crystallography and control of mineral morphology in desmids', *Proceedings of the Royal Society B: Biological Sciences*, 238(1292), pp. 203–221. doi: 10.1098/rspb.1989.0077.
Zhao, X. *et al.* (2019) 'Late-Holocene oceanic variability in the southern Benguela region driven by interplay of upwelling, fluvial discharge, and Agulhas leakage', *Holocene*, 29(2),

pp. 219–230. doi: 10.1177/0959683618810396.
Zonneveld, K. A. F. *et al.* (2010) 'Selective preservation of organic matter in marine environments; Processes and impact on the sedimentary record', *Biogeosciences*, 7(2), pp. 483–511. doi: 10.5194/bg-7-483-2010.